Screening Dynamic Phenotypes for Synthetic Biology

Felipe Perez

A thesis
in
The Department
of
Electrical and Computer Engineering

Presented in Partial Fulfillment of the Requirements
For the Degree of Master of Applied Science (Electrical and Computer Engineering)
at Concordia University
Montréal, Québec, Canada

May 2023

Concordia University

School of Graduate Studies

This is to certify that the thesis prepared
By: Felipe Perez
Entitled: Screening Dynamic Phenotypes for Synthetic Biology

Submitted in partial fulfillment of the requirements for the degree of

Master of Applied Science (Electrical and Computer Engineering)

complies with the regulations of this University and meets the accepted standards with respect to originality and quality.

Signed by the final examining committee:

_____Chair
Dr.

_____Examiner
Dr. Aashiq H. Kachroo

_____Examiner
Dr. Nawwaf Kharma

_____Supervisor
Dr. Laurent Potvin-Trottier

_____Supervisor
Dr. Steve Shih

Approved by_____
Dr. Zahangir Kabir, Graduate Program Director

Date_____ _____
Dr. Mourad Debbabi
Dean of Engineering and
Computer Science

To my sister who told a 12-year-old version of me that it was ok to like math :)

ABSTRACT

Screening Dynamic Phenotypes for Synthetic Biology

Synthetic Biology provides an avenue for reengineering the molecular machinery that make up cells. It has the potential of becoming a significant driver for discovery of new therapies and diagnostic methods. In fact, advances in molecular biology have made it easier to create large pools of edited cells, but there is a technological bottleneck to screen these cells to capture their phenotypes and link them to genotypes. Conventional screening technologies like well based structured arrays and Fluorescence-activated cell sorting (FACS) provide a means to screen genetically edited cells, but their current limitations prevent capturing dynamic phenotypes from mixed populations of edited cells. Microfluidic technologies provide alternatives that can be combined with timelapse microscopy to capture phenotypes. Paired with other techniques, these devices can provide ways to genotype mixed populations *in situ* and externally with single cell resolution. This work involves one of such techniques referred to as Single Cell Isolation Following Timelapse (SIFT), used to screen mixed libraries of synthetic oscillators. However, it is currently limited to *Escherichia coli* (*E.coli)* and further research is needed to adapt it to mammalian cells. As such, this thesis presents our implementation of the technique for screening reengineered *E. coli* cells in combination with an existing machine learning segmentation method referred to as Deep Learning Time-lapse Analysis (DeLTA). Similarly, this work features preliminary results to extend SIFT to Jurkat cells (human leukemic T cell line). In brief, the presented work involves the implementation of a microfluidic set-up to screen mixed populations of edited cells.

TABLE OF CONTENTS

LIST OF FIGURES

LIST OF TABLES

CHAPTER 1

Introduction

1.1. The Rise of Synthetic biology

Synthetic biology is an evolving field that holds the potential to develop new diagnostic tools [1], new treatments for diseases [2] and sustainable methods to make chemicals [3]. It revolves around the idea of applying computer science and engineering principles to biology. More specifically, it is a computational look as to how living organisms function. Cells can be seen as chemical computers with their own version of a source code. A code that is encrypted in nucleotides and stored in chains called Deoxyribonucleic Acid (DNA).

An algorithm referred to as the central dogma of biology is common across living organisms and is responsible of reading this code and turning it into chemical hardware. In brief, it works like a universal Turing machine, where a reader head walks along a ribbon containing input code. However, the biological version is more sophisticated. It has multiple "reader heads" running in parallel, which have rules guiding what should be read and when. The process takes DNA as input, transcribes it into Ribonucleic Acid (RNA) and then translates it into proteins. Then these proteins assemble to make more complex machinery, which allows the execution of routines like self-replication or input trigger cycles.

Advances in DNA reading [4] writing [5] and editing [6] technologies allowed us to hack cells and re-engineer them. The introduction of landmark genetic circuits such as the toggle switch [7] and repressilator [8] demonstrated that this is feasible. In fact, researchers have used these

elementary parts in practical applications. This is notably the case for the repressilator as demonstrated by T.Riglar *et al*. [9], where an upgraded version of the circuit was used to measure bacterial dynamics *in vivo* in a mammalian gut. Thus, giving researchers the ability to measure a process in vivo using an engineered organism. Having said that, the field is still at an early stage, and it is far from being able to achieve the same level of accuracy and precision that we have with electrical computers. There are a few technical barriers currently holding us back, but the one this thesis aims to address involves the need to understand the limitations of synthetic biological circuits by developing technologies to evaluate them.

1.2. The Need for Phenotype-to-Genotype Screens

The concept of phenotype is often used to refer to observable traits or characteristics of living organisms. The term encompasses a wide range of cellular properties that can be visually assessed or quantitatively measured such as cell morphology, gene expression, growth rate, doubling time, and spatial localisation of internal molecular machinery. Understanding how genetic information influences phenotypes is key to reengineer cells. Synthetic biology has been instrumental for this purpose by allowing researchers to develop fluorescent probes and intercellular controlling mechanisms.

Indeed, synthetic biology has a lot of potential, but as researchers create new biological circuits, there is a growing demand for ways to characterize their behavior. The development of techniques to make synthetic libraries of genetically altered cells has been on the rise. They are particularly useful in synthetic biology since they provide ways to make multiple variations of genetic parts with relative ease. However, there is a need for technologies capable of screening these libraries of cells to link phenotypes-to-genotypes [10]. The following section describes a few of those techniques along with their advantages and disadvantages.

1.2.1. Existing Cell Screening Techniques

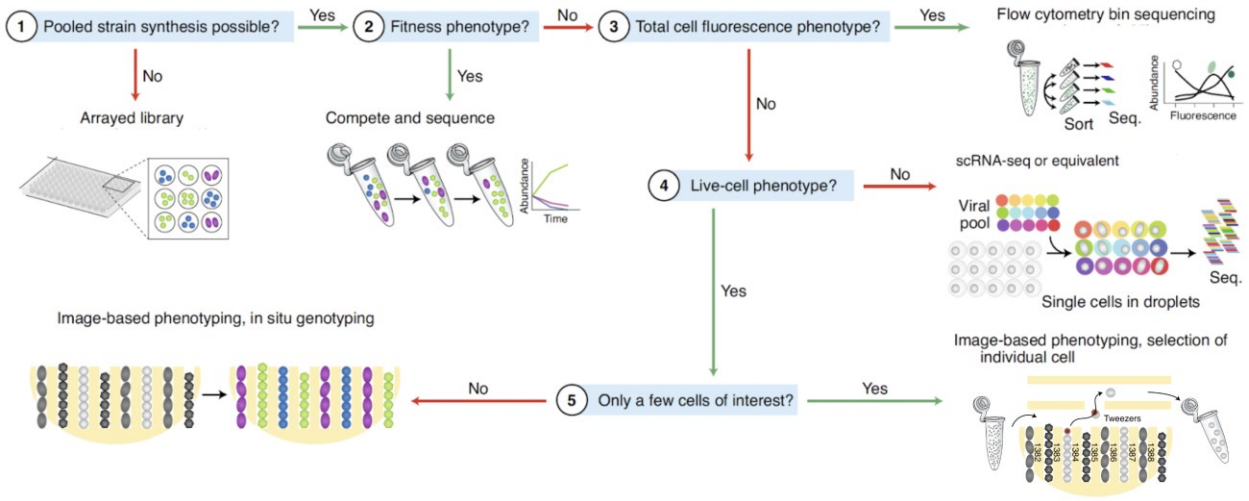

Figure 1 - Roadmap to method selection for library screening
Depending on how you answer the questions, different methods may be most suitable for your needs. Please see the text for a more complete reference list. (Adapted from [10])

Scientists have developed various methods to evaluate libraries of engineered cells, but choosing a technique to use is often based on trade-offs (Fig. 1). Well-based techniques can screen structured array libraries of edited cells by culturing known mutant strains into separate wells [11]. They can be imaged to capture phenotypes and sequenced to capture genotypes. However, this method is labor-intensive, and separating edited cells into wells poses a limitation. Mixed pool screening is preferred as it allows users to take advantage of pooled plasmid libraries, thus providing an easy method to generate random mutated plasmids in desired locations. To achieve this, different methods have been developed. For example, competition-based assays can screen engineered populations of cells using a selective pressure and a fitness phenotype [12], but this method constrains the types of phenotypes that can be evaluated. Fluorescence-activated cell sorting (FACS) is another method that separates cells into sub-populations based on a fluorescent readout , which can then be combined with bin sequencing to link phenotype-to-genotype [13].

However, the sorting is based on a single time snapshot measurement, making it difficult to capture temporal dynamics.

Other methods have sought to use recent advances in a field called microfluidics. In brief, it is the study of fluids at microscales, which have sparked the development of new kinds of devices. This knowledge has been instrumental for biological research by providing technologies to address common issues such as gene synthesis [14], plasmid assembly [15], and gene expression analysis [16]. As such, researchers have developed microfluidic methods for screening mixed populations of edited cells. One of these techniques is called Drop -Seq and it provides a means to capture the transcriptomic states from single cells[17]. The way it works is by encapsulating single cells with barcoded beads in droplets. When cells are lysed in the droplet, RNA strands hybridize with complementary sequences on the bead, thus capturing the expressed genotype at that time. One disadvantage is that cells are not kept alive, which prevents further phenotyping.

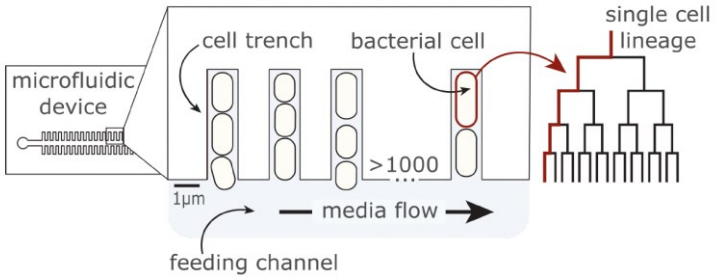

Figure 2 - Microfluidic device nicknamed the mother machine.
The "mother machine" microfluidic device traps individual rod-shaped bacterial cells in dead-end channels perpendicular to a larger feeding channel. As the cells grow and divide the old-pole "mother" cell remains trapped at the end of the cell trench while the newly divided cells are flushed away by constant supply of fresh media, allowing imaging of single cells over hundreds of generations. (Reproduced from [18])

To address this, scientists turned to microscopy and combined it with microfluidics to capture live-cell phenotypes using timelapse. Microfluidic devices provided ways to replicate cells' environments and geometries to culture them in an orderly manner. This is notably the case for the landmark device at the core of this thesis nicknamed the "mother machine". Its name comes from the ability to track *Escherichia coli (E.coli)* mother cells across multiple generations [19]. The way it works is by loading a pool of *E.coli* cells in the device and seeding them in trenches through centrifugal forces. Using a continuous flow of media, it is possible to keep cells alive with fresh media, while sending "daughter" cells to a waste beaker. The technique allows scientists to image 1,000s of monoclonal lineages of *E.coli* for multiple generations, making it a significant tool for capturing phenotypes.

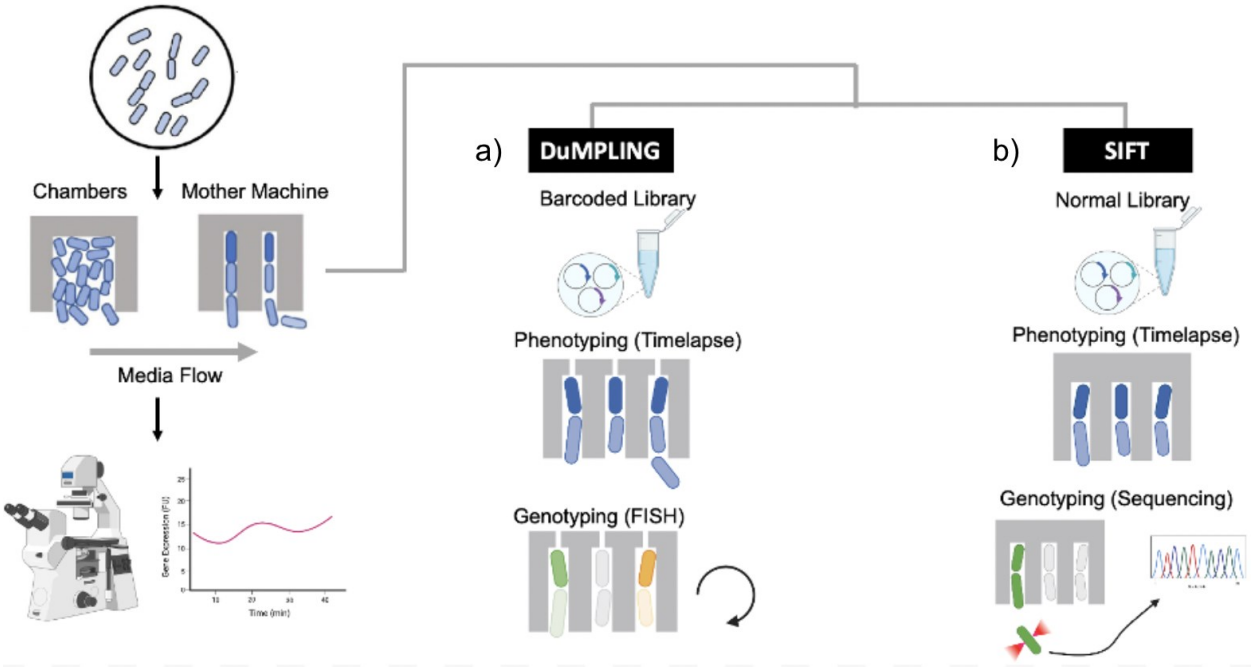

Figure 3 - Upgrades to mother machine devices to add genotyping abilities.
(a) Dynamic u-fluidic microscopy-based phenotyping of a library before *in situ* genotyping (DuMPLING). (b) Single Cell Isolation Following Timelapse (SIFT) (adapted from [20])

Two techniques have been developed using this device as a baseline to link phenotypes-to-genotypes in pooled assays. The first one is referred to as DuMPLING, which stands for **d**ynamic **u**-fluidic **m**icroscopy-based **p**henotyping of a **l**ibrary before ***in*** *situ* **g**enotyping . It involves using a modified mother machine with an extra back channel in combination with fluorescence in situ hybridisation (FISH) [21]. The method consists in three key steps: generating a mixed pooled barcoded library, characterizing its phenotypes with the mother machine, and detecting genotypes with rounds of FISH using fluorescent probes. The advantage of this technique is that it can perform simultaneous genotyping of multiple cells at once. However, it needs a barcoded library and cell fixation prior to hybridization, which removes the possibility for downstream growth and analysis. The second technique used to link phenotype and genotypes in pooled library assays is referred to as Single Cell Isolation Following Timelapse (SIFT)[22]. It is also based on a variation of the mother machine, which was complemented with pressurized valves. This method also relies on time lapse microscopy to characterize phenotypes of a pooled library, but it uses optical tweezers to isolate single cells that can be sequenced later. It has the benefit of screening mixed populations without DNA barcoding; however, only isolated cells can be genotyped. The screening power behind both methods is in their ability to accurately phenotype mixed populations of cells for multiple generations with single cell resolution under uniform conditions and providing a way to genotype cells. However, these methods are currently confined to rod-shaped bacteria, thus leaving room for further development.

1.2.2. The Current Technological Gap

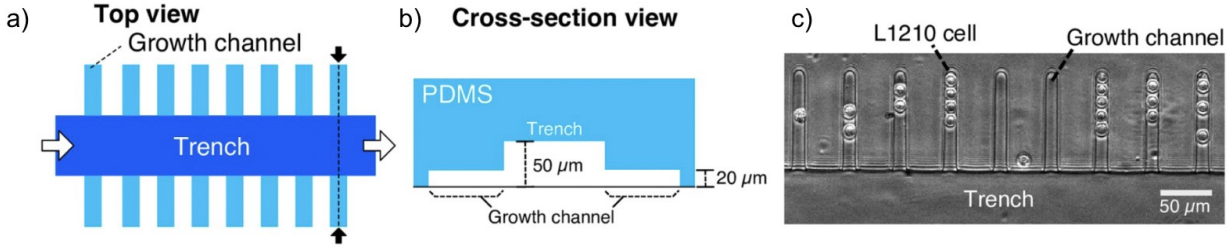

Figure 4 – Balanced growth of L1210 cells in the mother machine microfluidic device (a and b) Schematic representation of the device. (a) The top view of the device. The culture medium flows through the trench (white arrows). Cells trapped in the growth channels are observed simultaneously by time-lapse imaging. (b) Across-section of the device at the plane corresponding to the broken line indicated by the black arrows in (a). The height and the width of a growth channel are both 20 μm, which corresponds to the size of L1210 cells. (c) A micrograph of L1210 cells in the device. (Reproduced from [23])

Indeed, scientist have sought to expand imaged-based mixed population screening platforms to mammalian cells. In fact, the phenotyping capabilities of the mother machine have been extended to mammalian cells in two publications to date [23-24]. The most recent one investigates the intrinsic heterogeneity in the growth dynamics of mouse lymphocytic leukemia cells (L1210) and its relevance to anti-cancer drug susceptibility. However, this work has not been upgraded with genotyping capabilities thus far.

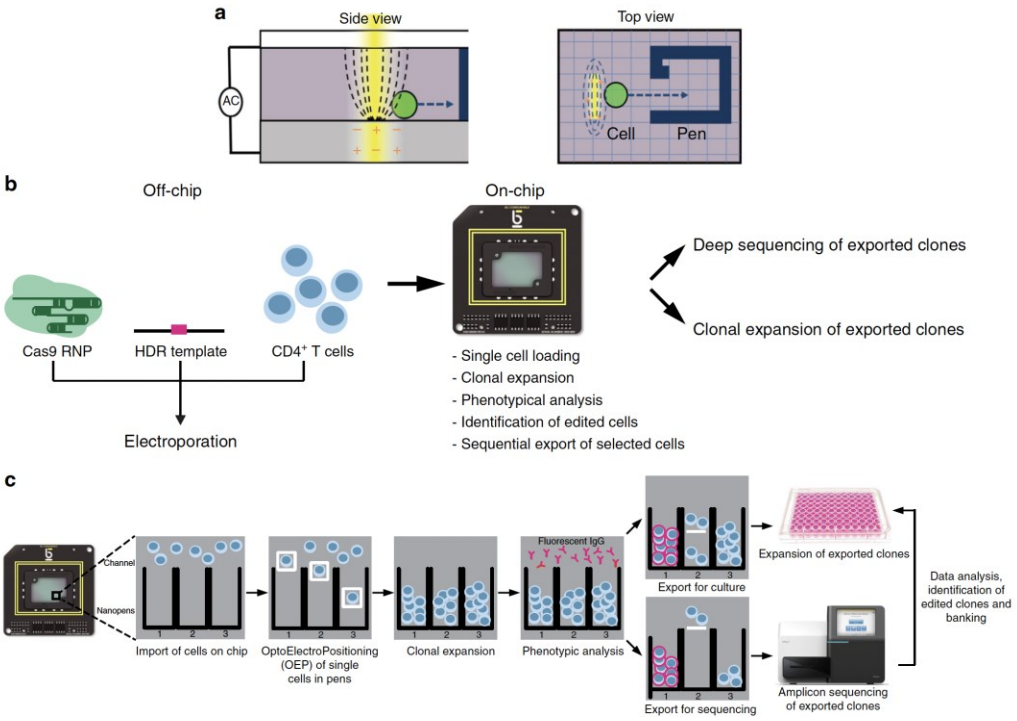

Figure 5 - Method to identify and select edited cell with high precision
a Schematic side (left panel) and top (right panel) views of the chip, depicting the OEP principle. A single-cell (green) is moved inside a NanoPen (blue solid lines, blue arrow) through OEP (yellow bar, dashed lines). **b**, **c** Schematic representation of the LACIS workflow. T-cell electroporation is performed off-chip, while clonal expansion, phenotype assessment, and export are performed on-chip. Each colony is split and exported. The first half of the colony is exported and further expanded through off-chip culture, while the remaining half is exported for validation through amplicon sequencing of the *CXCR4* locus. After on-target validation, the desired clones are selected for further expansion and banking (Reproduced from [25])

Other microfluidic efforts to screen mammalian cells include the development of Light-activated cell identification and sorting (LACIS) [25], which sparked the creation of a company called Berkeley lights. The technique is centered around a microfluidic chip that can perform single cell manipulation using light activated transistors that create a repelling electric field. Through their work in [25], this device was used to screen a pool of edited primary T cells aiming to identify the ones that had successfully knocked out a co-receptor for HIV. Despite its potential advantages, the complexity and cost of the chip remain significant barriers for widespread use.

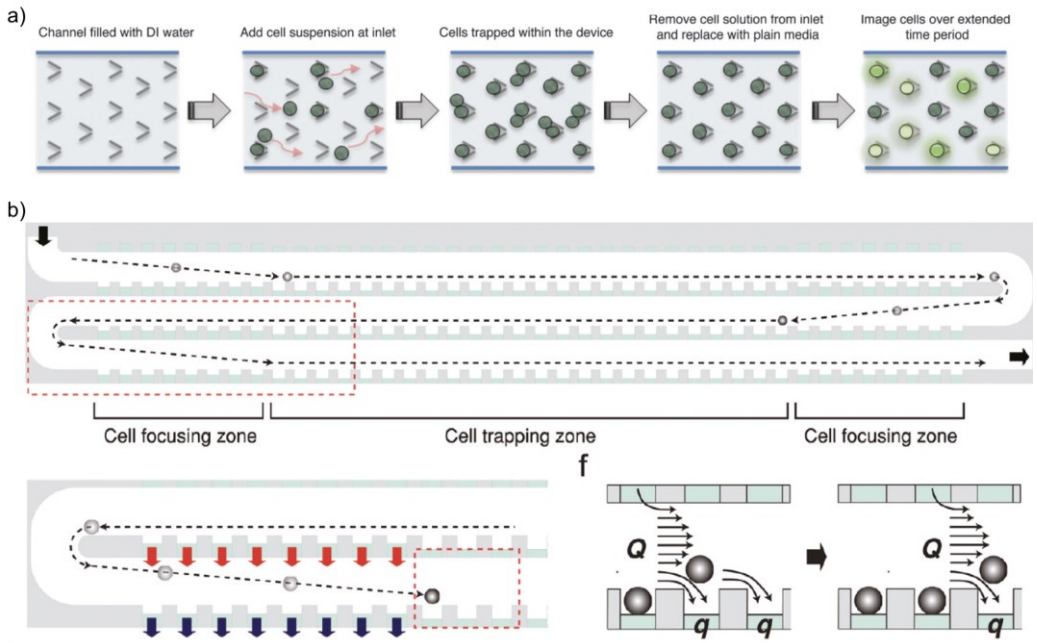

Figure 6 - Mammalian microfluidic devices with live cell phenotyping capabilities
(a) Schematic diagram of the protocol to trap single cells in the passive-flow microfluidic device from [26] (b) Schematic drawing of three columns of the array showing trajectory of cells in [27]. Cell suspension enters the array from the top left and exits at the bottom right. Dotted lines represent trajectory of cells. Boxed region in panel b showing cell focusing mechanism. Converging flow (red arrow) and diverging flow (blue arrow) through the dummy traps focus cells toward the traps.

Similarly, researchers have engineered other imaged-based phenotyping microfluidic methods, but their ability for genotyping potential still needs to be exploited. This is the case for a device introduced by Ramji *et al.* [26], which works a on passive flow to trap Jurkat T cells with a high retention rate over 12 hours of imaging. The study explored the impact of cell-to-cell variability on HIV activation using an HIV-GFP reporter. However, the microfluidic design relying on passive flow makes it difficult to change media conditions without dislodging cells from traps. In a similar manner, Chung *et al.* introduced in [27] a channel-based device to track cell-to-cell variability in intracellular calcium dynamics of Jurkat T cells. The retention of cells is done through a serpentine channel engineered with a series of traps to capture cells. This mechanism was optimized to allow for the trapping of up to 800 Jurkat Cells with a viability of 94% for at

least 24h. However, it still needs a means to genotype cells to be used as a mixed pooled screening platform. This brings us to the objective of this thesis that revolve around the need to provide screening capabilities for mixed pools of edited cells.

1.3. Thesis Objectives

This work builds upon the existing capabilities of the Potvin Laboratory to run microfluidic experiments with an *E.coli* mother machine. This thesis focuses primarily on the implementation of the necessary equipment to execute the SIFT technique to provide the laboratory with dynamic phenotyping abilities and a way to genotype cells of interest. In addition, this thesis explores the capability of expanding this technique to Jurkat cells. As such, I chose to divide the objectives in the following form :

1. The first objective of this work involves implementing the necessary equipment to perform mixed population screening through SIFT, while showcasing a practical application of the device.
2. The second objective of this work involves adapting the mother machine to Jurkat T cells to provide phenotypic capabilities.

1.4. Thesis Structure

The **second chapter** of this thesis discusses the implementation of SIFT as well as results gathered to meet the first objective. The **third chapter** of this thesis discuss the worked performed to meet the second objective with preliminary results adapting the mother machine to Jurkat cells. The **fourth chapter** presents a conclusion of what was achieved through this thesis. Lastly, the **fifth chapter** of this thesis is a collection of the methods used throughout experiments.

1.5. Author Contributions

This thesis project was conceived by Dr. Laurent Potvin-Trottier and Dr. Steve Shih. The template used to fabricate the microfluidic master molds for *E.coli* was based on the original SIFT files provided by Dr. Scott Luro [22]. Design for molds for mammalian cells was based on work from Giselle McCallum and Krista Jager. *E.coli* strains and plasmid construction were completed by Paige Allard and in support with Fotini Papazotos. It is important to acknowledge the implementation of a DeLTA analysis pipeline performed by Hans Olischlager, upon which I build on to analyze my results for SIFT work. The microfabrication, microfluidic and optical set-up constructions as well as experiment execution and analysis in this work was completed by Felipe Perez.

CHAPTER 2

Single Cell Isolation Following Timelapse (SIFT)

In this chapter, we begin with a brief description of the design and manufacturing process for our E.coli microfluidic device. We discuss the implementation of a pressure and optical system necessary to execute the technique. Next, we introduce two mock-up assays demonstrating the potential of the technique as well as preliminary results in a synthetic biological application. Lastly, we discuss the remaining challenges and future work to perfect this technique.

2.1. Screening *E. coli* Populations with Single-Cell Resolution

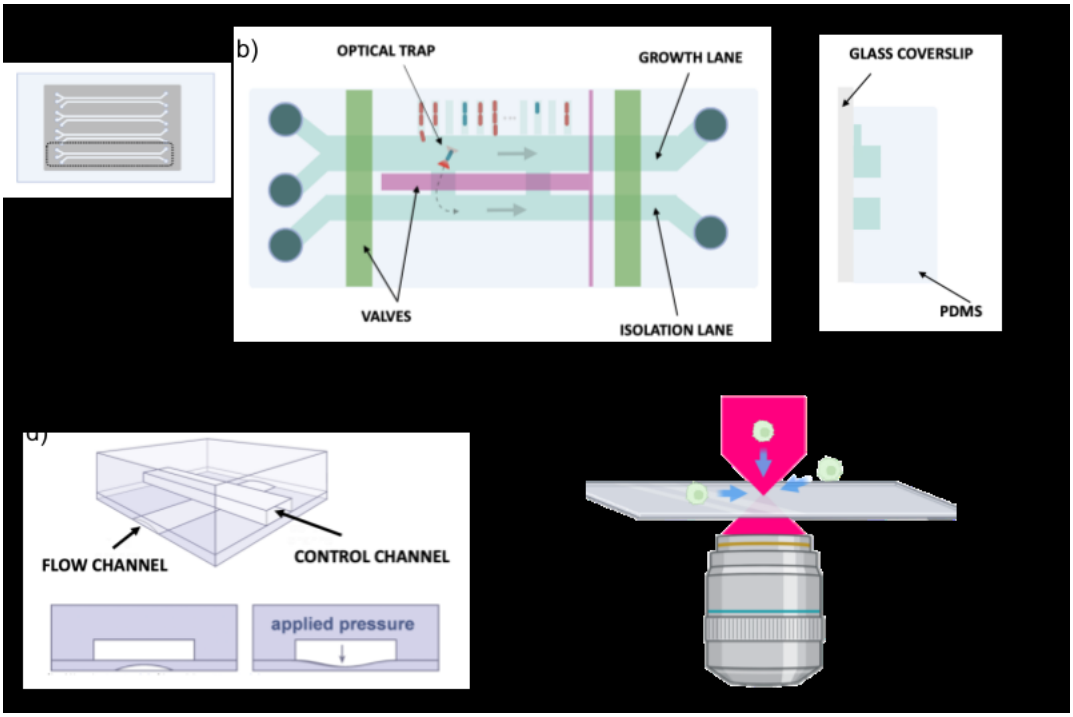

Figure 7 – Microfluidic platform for single cell timelapse and manipulation
(a) Top view of the device presenting four set of lanes. (b) Close-up view on one set of lanes showcasing the key elements. (c) Side cross-section view from the device showing the PDMS chip bonded to a glass coverslip. (d) Schematic showing the method to close and open valves [28]. (e) Schematic showcasing optical tweezers trapping a cell.

The design for the microfluidic chip implemented by this work was gifted by Dr. Luro and first published in [22]. It features the core geometry of the mother machine introduced in section 1.2.1. The device can culture thousands of monoclonal lineages of *E.coli* across several generations. Using a continuous flow of media provides fresh nutrients and gets rid of undesired cells by flushing them to the outlet. Timelapse of the device with edited cells using a fluorescent reporter allows users to track gene expression overtime across multiple generations. The high-throughput phenotyping capabilities of the device is due to the scalability of the features and the small size of cells. The microfluidic chip for SIFT is made of four growth channels referred to as lanes, with each lane hosting several thousand trenches. Using a 63X Plan-Apochromat objective lens, each lane can be imaged in sets of 55 trenches per position. This enables the tracking of up to 15,600 mother cells per experiment. While the experiments presented in this thesis used a single channel for simplicity, the potential for high-throughput screening is significant.

The high-throughput capabilities of the mother machine are well-established [29], but this work implements an upgraded design that includes features enabling the isolation of single cells. To achieve this, small junctions connect each growth lane to an isolation lane, with push-down (Quake) valves [28] controlling the flow between them. These valves use a flexible PDMS membrane that collapses when pressurized, allowing them to be opened or closed as needed. In addition, valves are also located at the inlet and outlet of each growth and isolation lane, serving multiple purposes. The valves enable cleaning procedures, which are necessary to remove biofilm at the inlet of the growth lane to prevent complications. They are also necessary to stop the flow across the growth lane, while isolating cells. This is due to the method for cell manipulation used by SIFT, commonly referred to as Optical Tweezers or Optical Trap [30-31]. The technique

involves using a high-power laser focused with a state-of-the-art microscope objective. When the beam is aimed at a cell, it creates an attractive force that keeps the cell at one location. By moving the geometry around the cell, it is possible to transport it to a new location on the chip.

2.2. METHODS

2.2.1. Microfabrication for the Device

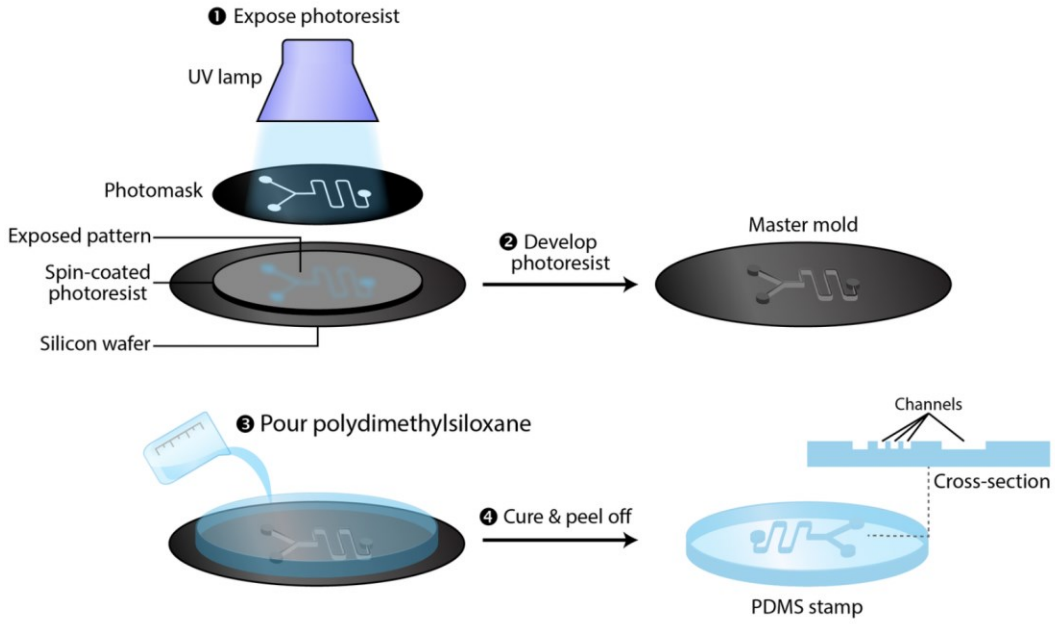

Figure 8 – Microfabrication process for microfluidic devices
Steps 1-2 are referred to as photolithography and steps 3-4 are referred to as soft lithography. (Reproduced from [32])

The microfabrication process of the mother machine involves multiple steps using different techniques and spanning more than 4 days. First, an array of microfluidic chips is designed using a common 2D drawing software like AutoCAD. Then two main techniques are used to manufacture the chips. The first one is referred to as photolithography. It is a technique that uses the designed pattern on a mask to create microstructures on a silicon wafer by coating thin layers of photoresist and exposing them to light [33][34][35]. The second technique is known as soft lithography, and it involves using the master mold to cast the actual microfluidic devices on Polydimethylsiloxane

(PDMS). This is a common material used in microfluidics as it is gas permeable and biocompatible [33].

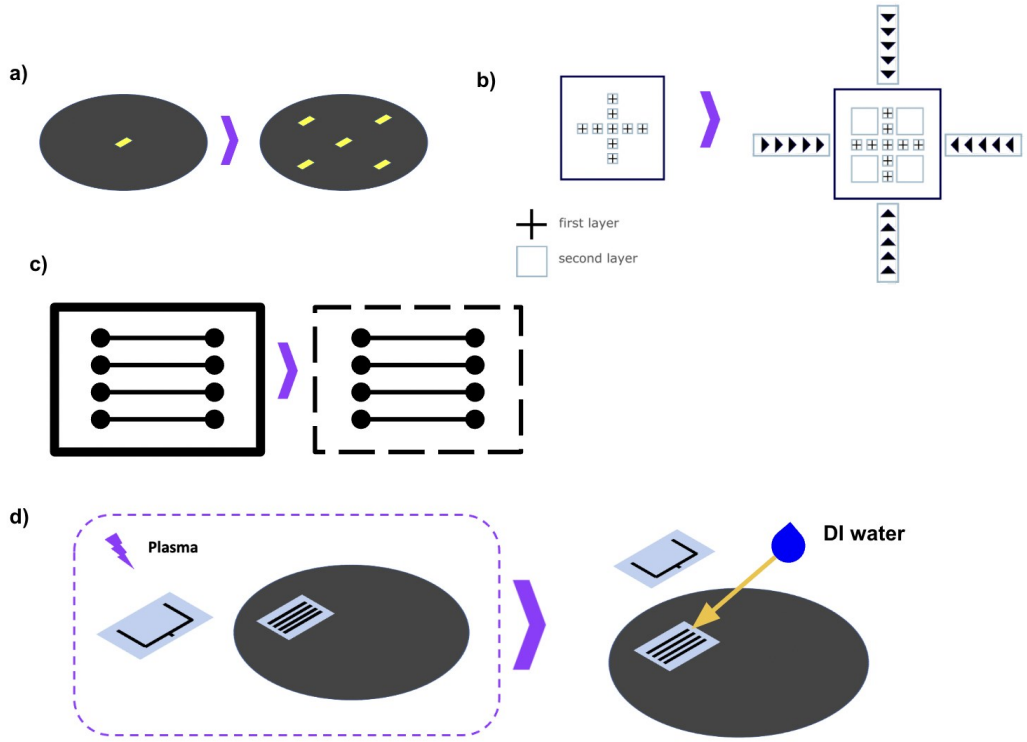

Figure 9 - Improvements to wafer design and fabrication process
(a) Added markings for probing spin coated layer heights. (b) New design for alignment marking significantly improved the manufacturing process. (c) Microfluidic chip outline modification to prevent connecting lanes from poor punching. (d) New step introduced for manufacturing the multilayer PDMS chip. It allowed alignment corrections between layers, which was not possible before.

Contributions from this Thesis to Mask Design and Chip Manufacturing

The mask design for the SIFT mother machine was inherited from Dr. Luro's work published in [22]. In this work, I updated the wafer design with improved markings to measure the height of each layer at various points in the wafer. This proved to be very useful to troubleshoot uneven thickness coating issues, which previous versions were lacking (Fig. 9a). Similarly, in collaboration with Krista Jager and Giselle McCallum, I introduced a new design for alignment

marks used in multiple layer microfabrication, which greatly simplified the process (Fig. 9b). In terms of microfluidics design, I optimized the location of inlets and outlets to provide increase the clearance for punching holes. Likewise, I upgraded the outline of devices from a plain line to a dashed one, which was necessary to avoid lanes connecting to one another in case of poor punching (Fig. 9c). Lastly, different trench widths were added in the wafer array for testing purposes. It should also be noted that this thesis improved the existing fabrication method for the microfluidic device by providing a different method to bond PDMS to PDMS layers similar to [36]. The method consisted of using a plasma cleaner to activate the surface of the material and prior to bonding adding a droplet of deionized (DI) water to allow alignment adjustments (Fig. 9d) .

2.2.2. Implementation of a Pressure System to Control Push-Down Valves

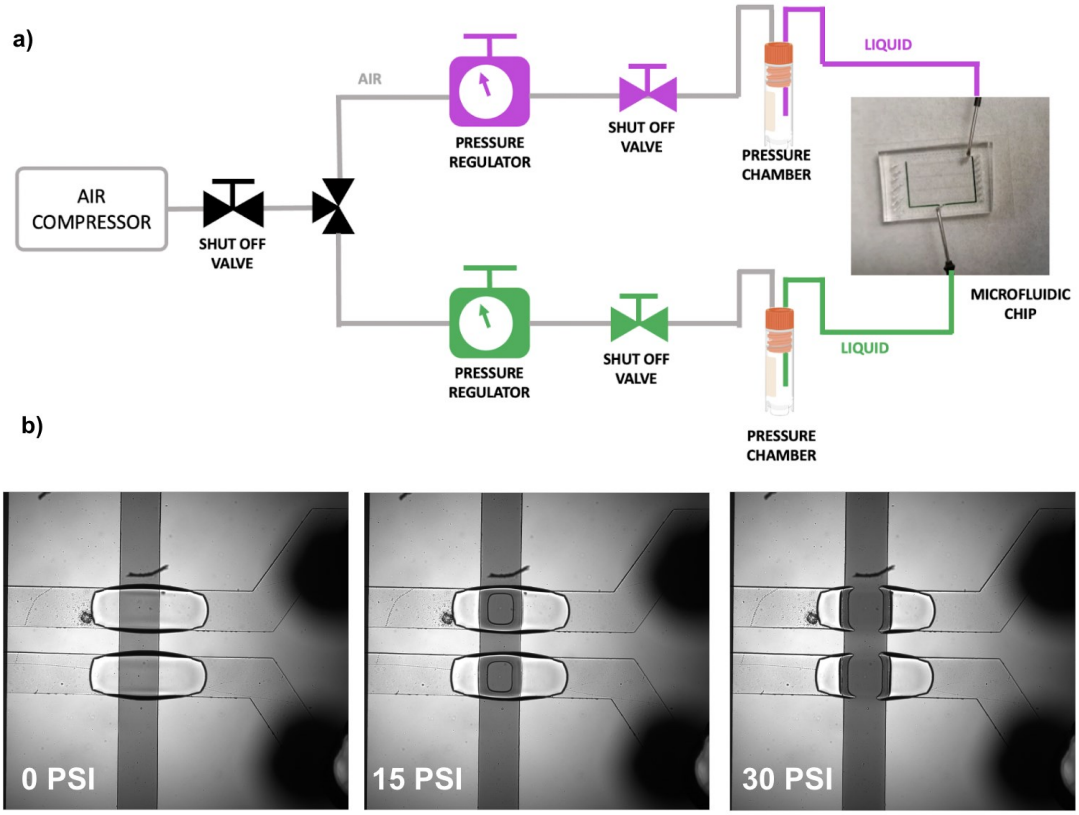

Figure 10 – Pressure set-up to operate microfluidic push-down valves.
(a) Schematic presenting the pressure set-up, which uses a generic compressor as the air supply and a combination of valves and regulators to precisely control pressure. Pressure chambers switch the fluid from air to dyed water to prevent losing pressure from the gas permeability of PDMS. (b) Microscopy images showcasing the closure of valves at 30 PSI.

Through this work, we developed a pressure system to precisely control the operation of push-down valves. This paragraph describes the implementation of the pressure set-up. To power the system, we opted to use a generic air compressor to avoid relying on building-supplied air pressure. This also allowed us to have a portable set-up, which proved to be useful given the logistical challenges posed by having a wet lab and microscopy room at different locations. To ensure that inlet and outlet valves opened and closed at different times than the ones between lanes, it was necessary to have two independent outputs. We achieved this by using a combination of shut off valves, diverting valves, and precision air regulators, which were like those in [37]. As

PDMS is a gas-permeable material, liquid actuating valves were preferred. To switch from air to liquid, chambers inspired by [38] were engineered to enable pressurized air to move the liquid into the control channels and perform the actuation. We used DI water with food colorant as a controlling liquid, since it provided a visual indicator in case of leaks. To close the valves, the pressure was increased gradually to reach 30-35 psi (Fig. 10b). To reopen them, we simply released the pressure and allowed the system to stabilize with atmospheric pressure. By keeping the air compressor ON, it was possible to keep valves closed indefinitely. Overall, this custom-made implementation proved to be sufficient to meet the necessary pressure requirements for push-down valve actuation.

2.2.3. Implementation of Optical Tweezers for Single-Cell Isolation

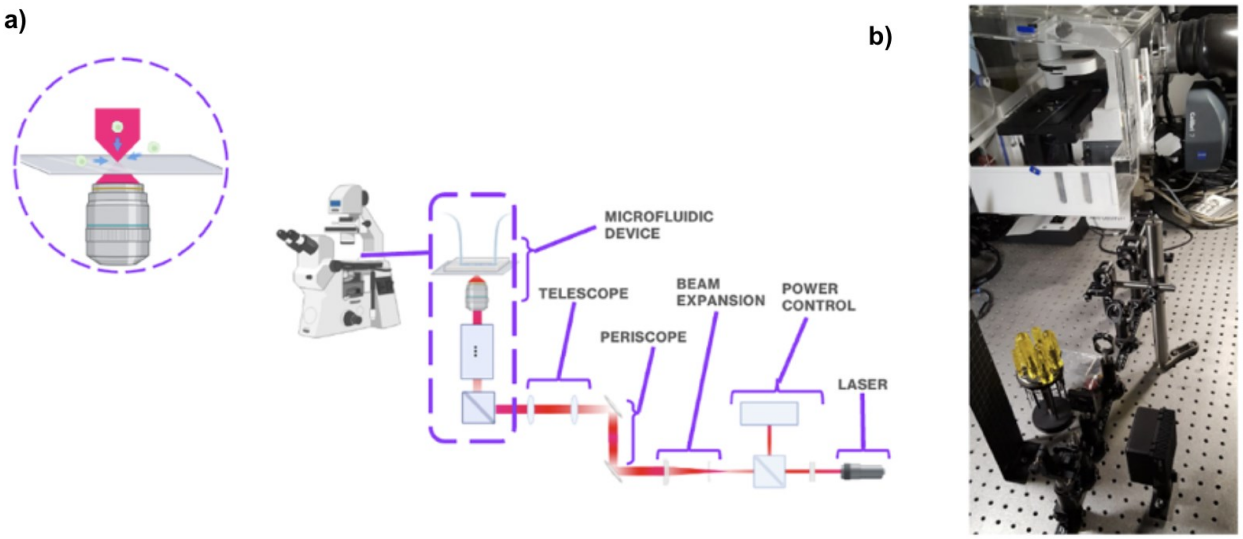

Figure 11 – The set-up designed for our optical tweezers
(a) Schematic of the set-up to achieve cell isolation. A laser is passed through a series of optical elements to control the power, diameter and collimation of the beam aimed at the microfluidic sample. (b) Image of the physical set-up aligned at the microscope port.

In this section, we describe the successful implementation of Optical Tweezers to isolate live cells by building upon existing methods from [22, 39]. The guiding principle behind optical tweezers is that when light passing through a medium hits an object, it generates a force called radiation pressure [31]. It is possible to make this force strong enough to trap a living cell in space. This can be achieved by focusing a powerful laser into a narrow beam. Different ways of using this principle exist, but the way it is employed in this work is to manipulate single *E.coli* cells in space.

The light source used for this implementation was a continuous wave ytterbium laser with a wavelength of 1,064 nm, which was chosen to mitigate the impact that the beam might have on cells [40]. The laser could achieve 10W of power, but we operated at around 2W and diverted more than half of this power to a beam block. This strategy was used to damp fluctuations in power coming from the laser source. Following power attenuation, the beam was passed through a series of optical elements to adjust its diameter and steer it until it reached the microscope objective. A 100x APO oil objective with a high Numerical Aperture (NA- 1.49) was used to focus the laser at a narrow region, thus achieving a stronger trap. The force holding the cell was also influenced by how well the laser was aligned and the amount of power going into the microscope. The laser steering in the XY plane was achieved by a set of mirrors in a periscope, which brought the beam to the appropriate height. The steering of the focal point of the trap in the Z direction was achieved with a set-up called a Keplerian telescope (see Fig. 11). In brief, two convex lenses are placed in series and by controlling the spacing between it is possible to impact the focal point for the exiting beam. Upon alignment, the operation of the trap simply consisted of aiming the laser beam at a cell to hold it in place, while the XYZ stage moved the chip.

Contributions from this Thesis to The Optical Set-up

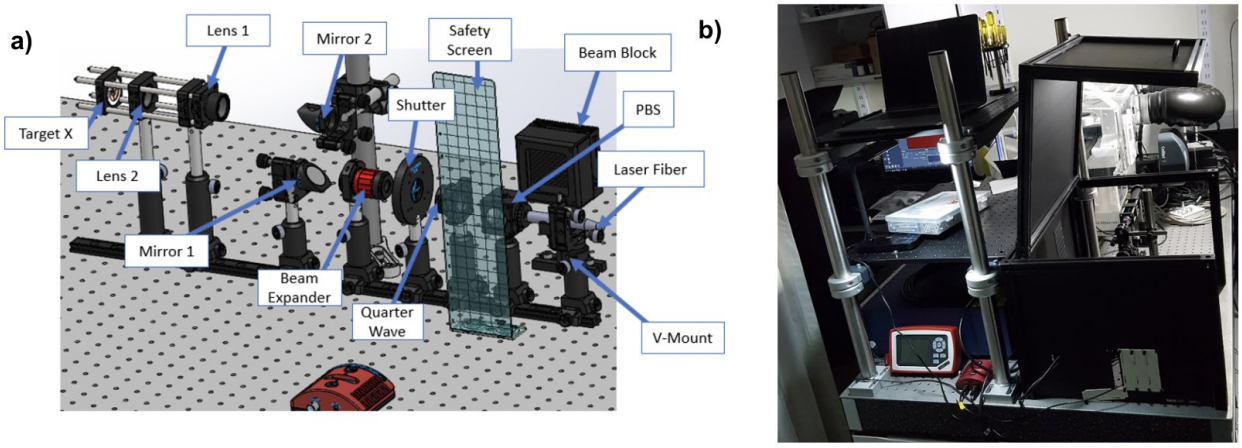

Figure 12 – Design of the set-up with necessary components to accommodate existing space (a) Computer-Aided Design (CAD) from Solidworks showcasing components chosen from Thorlabs prior assembly. (b) Constructed optical enclosure for operating the laser safely and shelf to support syringe pumps needed for the microfluidics set-up.

Although the design for an optical trap was introduced by the original SIFT paper [22], it required a significant amount of engineering work to implement it. Indeed, the paper provided information on the key optical components like the lenses, beam splitter or beam expanders to use, but I chose the optomechanical components to construct the set-up. The trap was built in a rail system to allow a flexible alignment with our microscope. An enclosure was designed and built around the trap for safety purposes. Similarly, to accommodate for the space taken by the optical set-up, I engineered a custom-made storage shelf for the placement of syringe pumps.

2.3. RESULTS

2.3.1. Mock-up assay validates the screening potential of the microfluidic chip

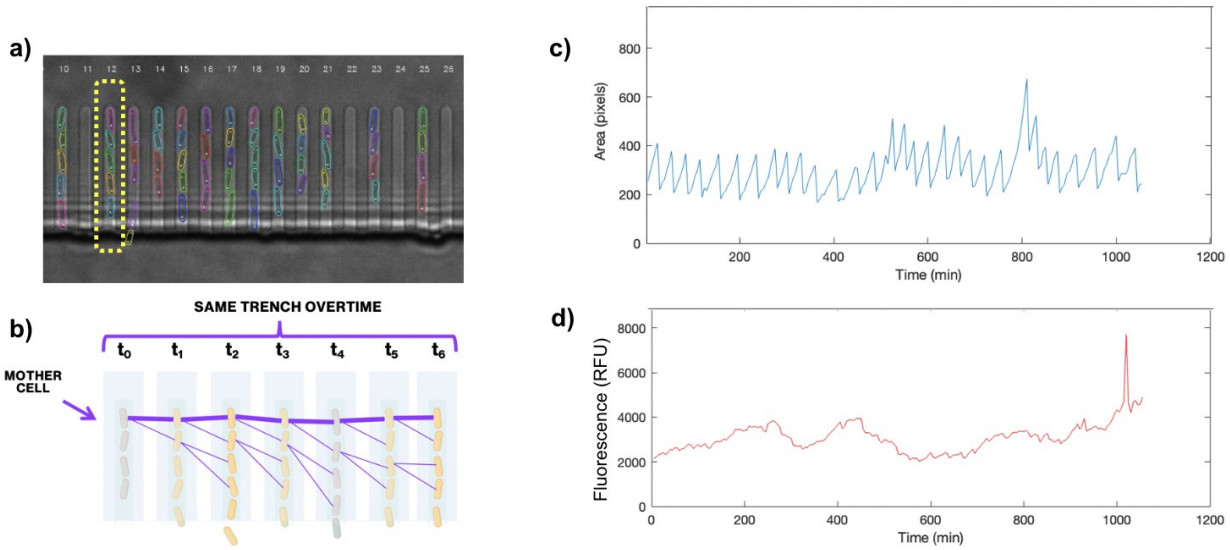

Figure 13 – Throughput test to capture dynamic phenotype for multiple cells
(a) Image of cells segmented in this experiment using the machine learning algorithm DeLTA published in [41] and a constitutive RFP expressing *E.coli* strain.(b) Schematic portraying the tracking capabilities of the segmentation pipeline. The top cell in trenches referred to as the mother is tracked across multiple divisions. (c) Time trace for the captured area of a mother cell. Peaks represent the division of the cell. (d) Mean fluorescent signal capture for the mother cell throughout the experiment.

The microfluidic device presented in this work successfully tracked the gene expression of *E.coli* cells over multiple generations, revealing significant potential for screening capabilities. As a throughput test, we loaded a lane of the microfluidic chip with a population of *E.coli* engineered to express red fluorescent proteins (RFP) constitutively. We imaged the chip at various positions for 17 hours at an interval of 5 min between frames. We then took this series of images and fed it to a deep learning algorithm referred to as DeLTA [41], that was able to segment and track cells using the fluorescent signal from cells (Fig. 13a,b). The output from this algorithm was then used to extract key metrics for mother cells in the mock-up population. One of the parameters observed was the change in area of a cell over time (Fig. 13c). This allowed us to establish when divisions

were occurring for a particular mother cell. We could also track the average fluorescence of a cell through time, thus making a time trace estimate of the gene expression for that cell (Fig. 13d). This becomes particularly handy when one is developing a gene circuit and requires characterization of its behavior over time. The true advantage of the mother machine is that these parameters can be extracted for several lineages. For example, in this assay, we tracked 418 lineages for an average of 32 generations, which is significant but represents only ~5% of what we could potentially track per experiment at max capacity. To sum up, our findings demonstrate the high-throughput phenotyping potential of this microfluidic device along with its ability to track gene expression over time.

2.3.2. A mock-up assay demonstrates proof-of-concept cell isolation.

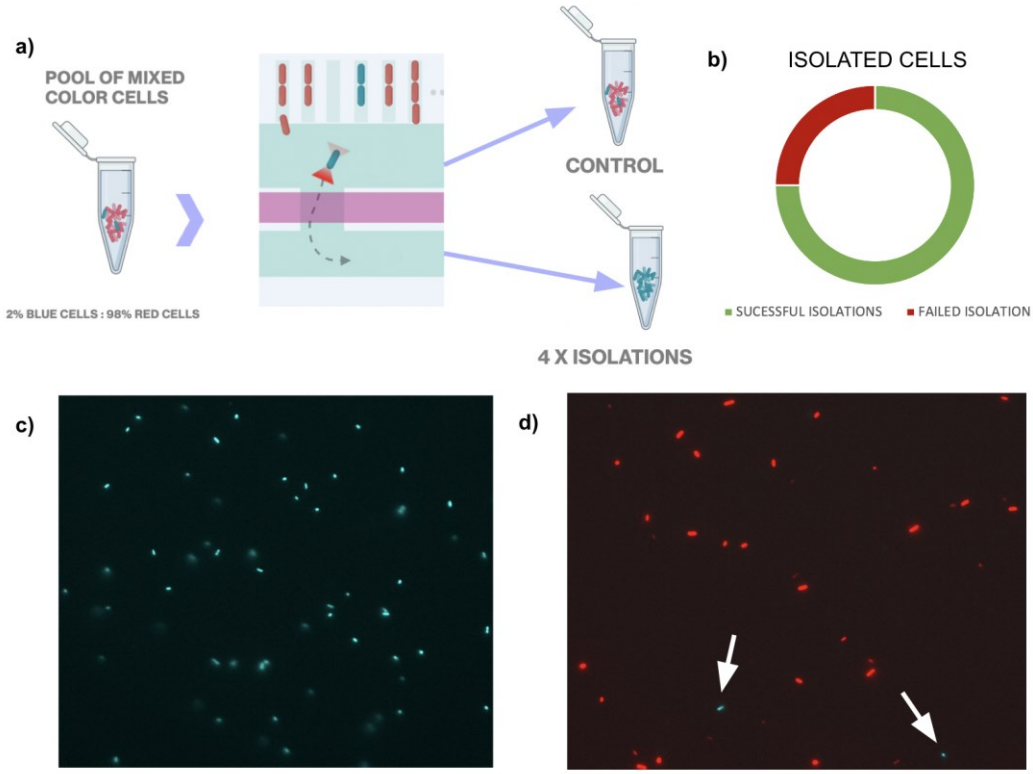

Figure 14 – **Mixed pool mock-up cell isolation assay**
(a) Schematic showing the general idea of the assay. Using a mixed population of 98% of cells expressing RFP and 2% of cells expressing CFP. Four isolations were performed to extract CFP expressing cells in a 96-well plate and grown overnight. A mixture of the imaged lane was collected as control. (b) Graphic depicting three of our isolations were successful. The failed one is suspected to be a manipulation error. (c) Sample of one of the successfully isolated wells after 24h, imaged in between two coverslips. (d) Sample of the control well after 24h .

After validating our device's potential for screening phenotypes, we proceeded to test its isolation capabilities. We performed a mixed population mock-up assay with a ratio of 98% of cells expressing RFP to 2% expressing CFP and imaged it for 17 hours. However, it is important to mention that the loading was achieved with an alternative method than the one published in [22]. In brief, the chip was loaded with cells and the lane was left to dry, which stresses cells, makes them smaller and placed them in trenches. It was possible to bring them back to a growing phase by flowing imaging media at 5µL/min. The reason for this was that loading with the

conventional method was unsuccessful. Following this, we proceeded to isolate four cells expressing CFP in four separate wells (Fig. 14a). This was achieved using the laser at a power of 60 mW, which is 4 times the value used in the original SIFT paper [22]. The higher required power was likely due to the alignment of the laser that could be further optimized. A mixture of cells from the growth lane was collected in a fourth well as a sample of the mixed population for control purposes. The 96-well plate was then incubated overnight at 37°C. To evaluate the quality of our trapping in the 96 well plate, we placed 1 µL of each well in a coverslip and observed it under the microscope. The results indicated that three out of our four isolated wells had successfully grown into a uniform culture of CFP cells (Fig. 14b,c). The empty well was likely due to a manipulation error as it was the first isolation. The control well accurately displayed a mixture of red cells in majority with a very small number of blue cells (Fig. 14d). Overall, this assay demonstrated that it is possible to isolate 1 cell among a mixture of cells and start a new colony from this individual.

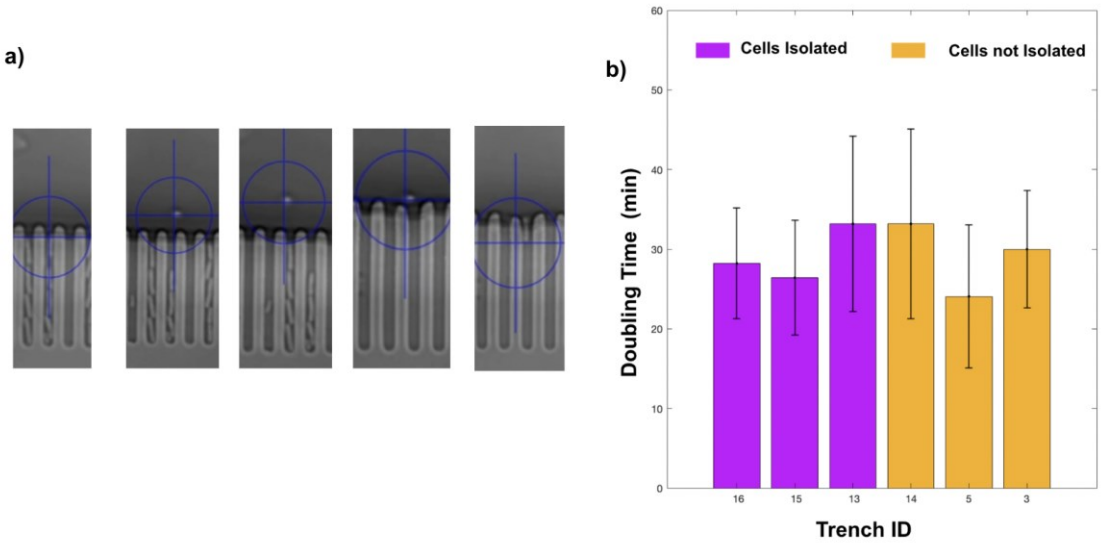

Figure 15 - Cell isolation preliminary assessment
(a) Images depicting cells subjected to optical trapping and loaded into new trenches. These cells were then imaged again for 13h along with non-manipulated cells. (b) Graphic depicting the time it takes for cells to divide comparing 3 cells that were optically trapped with 3 cells that were not.

While keeping the chip running, we used the optical trap to seed three trenches with cells exposed to the same duration of trapping as the ones in the wells and imaged them for 13 hours. To quantify the impact of optical trapping, we used the timelapse of trenches seeded with the laser and compared the doubling time of isolated cells with neighboring cells as a control (Fig. 15 a,b). It is difficult to conclude the impact of trapping just from this assay due to the stress the dry-loading method could have on cells. Nonetheless, this sanity check suggests that trapping shows no apparent fitness impact. It is important to mention that a similar test was carried in the work by Dr. Luro and no apparent impact was detected. Having said that, more testing should be conducted with higher power settings or exposure times to understand if there is a condition that can kill cells due to phototoxicity or local temperature changes.

2.3.3. Preliminary screen for a pool of oscillating genetic circuit

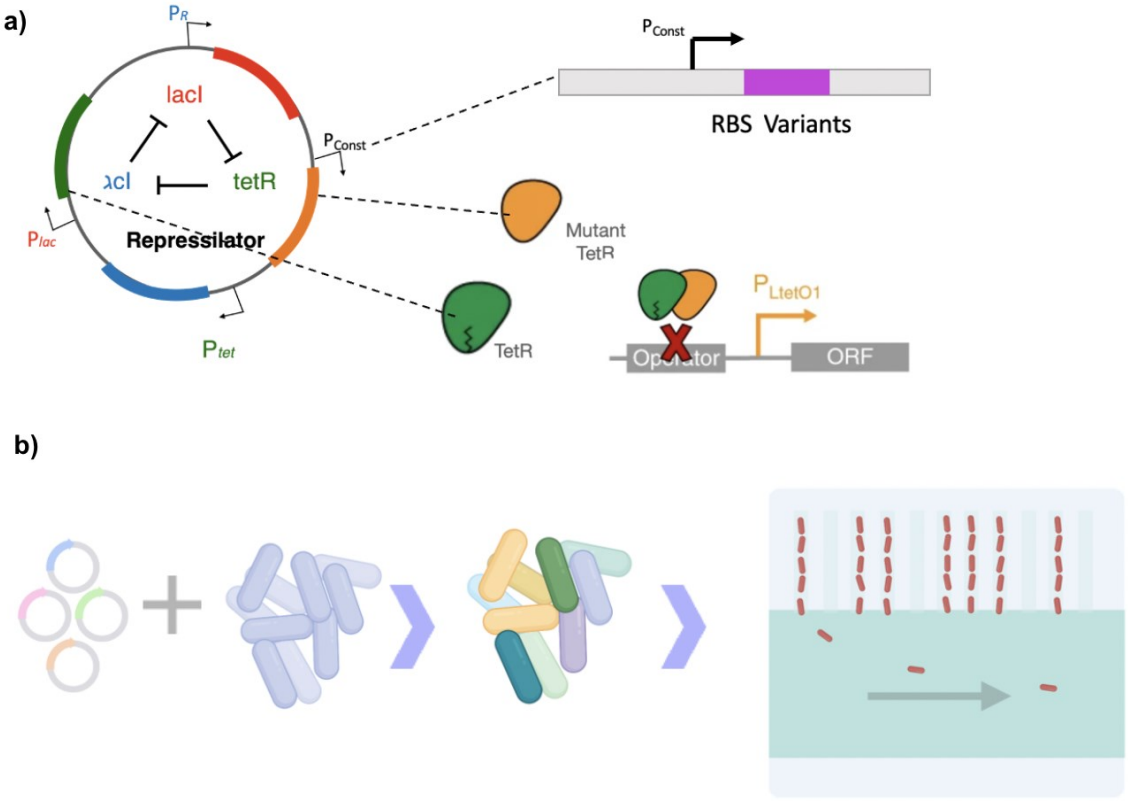

Figure 16 – Practical application of the screening method
(a) Image depicting the dominant negative repressilator used in this experiment. Using three genes repressing one another this genetic circuit generates oscillations with a period spanning multiple generations. The dominant negative version features a mutant TetR that dimerizes with the wild type to control the period of oscillations. This assay utilizes a library of variants produced from the optimized *SL229* circuit in [22]. (image adapted from [22]). (b) Schematic depicting the process. The plasmid library was generated by Page Allard and the phenotype screening was performed by me.

In this assay, we wanted to test our set-up on a practical experiment. This work was done in collaboration with Paige Allard, a master's candidate in the Potvin laboratory. Her work explores characteristics of synthetic oscillating circuits. More specifically, it uses a circuit called the repressilator, which is a multigenerational oscillator. It consists of three repressor genes (Tn10 TetR, bacteriophage λ CI and *E. coli* LacI) arranged in series to make a delayed negative feedback loop [8]. In this case, an altered version of this circuit was used referred to as the Dominant Negative (DN), which has a mutant TetR that dimerizes with the wild type, thus preventing it from

being active in the circuit. This process provided scientists with a means to control the repression thresholds by tuning the expression of TetR. In fact, that is what Luro *et.al* showcased in [22], the author constructed a library of cells expressing varying levels of the mutant TetR. Then using the microfluidic set-up, he screened for the most precise oscillator, that is the one that is optimized to keep its period constant.

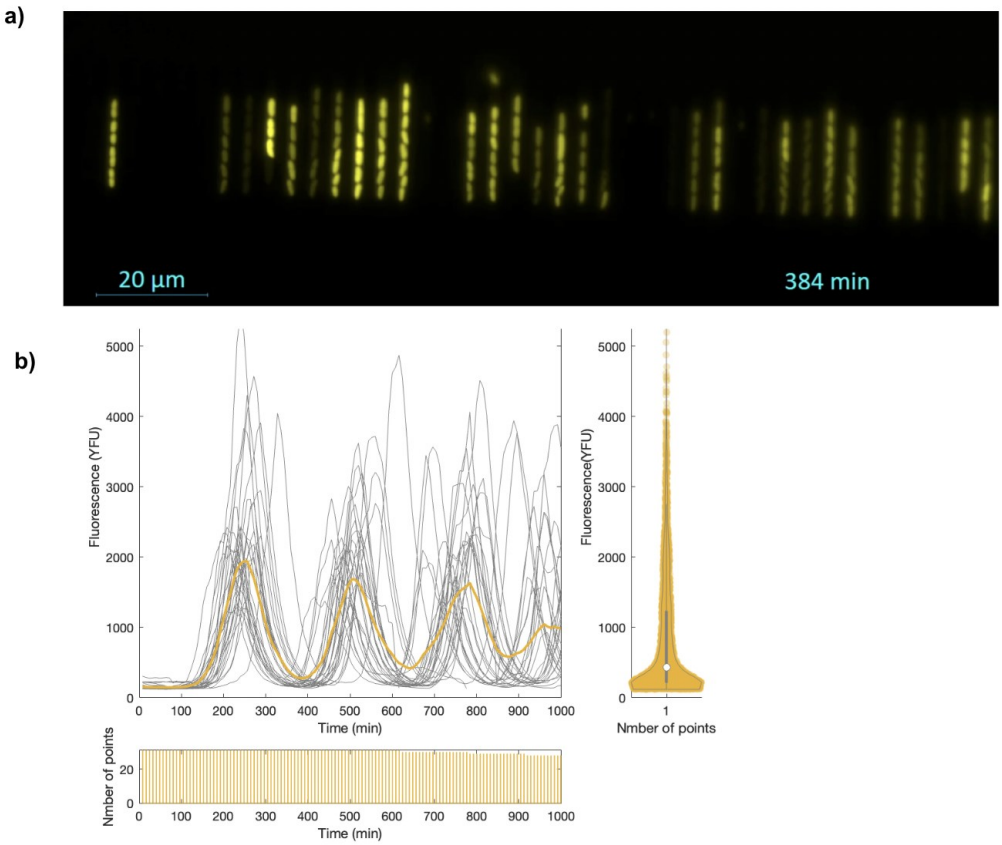

Figure 17 – Pool of oscillating imaged and phenotypes
(a) Image showcasing cells from the library oscillating in the SIFT mother machine used in this assay.(b) Captured time traces for the oscillating circuit using YFP as a fluorescent signal. Non-oscillating cells were excluded from this graphic for simplicity.

The work carried in this assay utilizes this optimized oscillator gifted by Dr. Luro. Building from this circuit, we sought to mutate it again to identify even more precise oscillators. To achieve this, we generated a pool of mutants by varying the RBS region through error prone PCR. Then,

we loaded it into our microfluidic device and imaged it for 16 hours (Fig. 17a). Challenges with stage jitter, prevented us from segmenting the data at the time of the experiment. In addition, biofilm build-up in the growth lane prevented us from isolating single cells. Nonetheless, in a post experiment analysis, we removed jitter from the timelapse and manage to track up to 73 mother cells, out of which 30 were oscillating. Not ideal, but good enough to plot the various oscillations captured by our set-up (Fig. 17b). Through this experiment, we were able to obtain preliminary results for oscillating circuits and identify key challenges to focus on to achieve a successful screen.

2.4. Challenges Remaining and Future Work

Overall, our experiments demonstrated that through the implementation of SIFT, it is possible to find a single cell from a mixed population, isolate it and grow a new colony from it. However, two challenges need to be addressed to truly exploit this screening potential. The first one involves troubleshooting issues of poor loading, which limits the number of cells we can image. The knowledge gathered from these assays suggest that the trench height of our microfluidic chips is small for the strains we worked with as they had difficulty entering their trenches in the original loading by diffusion method used in [22]. This could be an artifact of the master wafer used, indicating that it might need a bigger height. It could also be the multilayer soft lithography process, which still needs optimization. The second challenge relevant for screening is to make our segmentation code more flexible so that the analysis can still proceed even if the experimental set-up is not ideal. This can be done by training the machine learning algorithm on imperfect loading conditions and space jitter so it can identify better cell traces. Similarly, to further advance the ability to isolate cells, strategies to prevent biofilm

formation in the growth lane should be explored. Lastly, different approaches to simplify the manufacturing, tubing set-up and experimental procedure should be explored to reduce sources of error and simplify SIFT assays.

CHAPTER 3

Screening Dynamic Phenotypes in Jurkat T Cells

In this chapter, we introduce the motivation behind this work. Next, we introduce our microfluidic device and the experimental setup employed throughout our research. Finally, we present three preliminary results that establish a foundational baseline for the development of a Jurkat mother machine.

3.1. Motivation for a Jurkat mother machine

In this part of the thesis, we are prototyping a device to phenotype Jurkat T cells. Cell phenotyping in Jurkat cells is generally done in bulk measurements through techniques such as FACS. They have been instrumental for multiple discoveries, but there is a need to increase the precision of these measurements to single cells and to track these phenotypes overtime. The work presented in this section, aims at addressing this need by adapting the microfluidic device known as the "mother machine" to Jurkat cells (leukemic human T cell lineage). A successful development of such a device would pave the way to a mixed pool screening platform. Similarly, it would unlock a new method to track gene expression overtime for single Jurkat T cells. In fact, there is a precedence for adapting the device to other organisms like *Corynebacterium glutamicum* [42], *Bacillus subtilis* [43] and *Saccharomyces cerevisiae* [44]. Other groups have adapted the device to mammalian cells [23-24] . This research is of particular interest for scientists seeking to understand the internal mechanisms of T cell lymphocytes using Jurkat cells. In addition, it is

relevant for users seeking to characterize existing synthetic biological circuits or engineer new ones in T cell lymphocytes.

3.2. METHODS

3.2.1. Microfluidics Design for a Jurkat mother machine

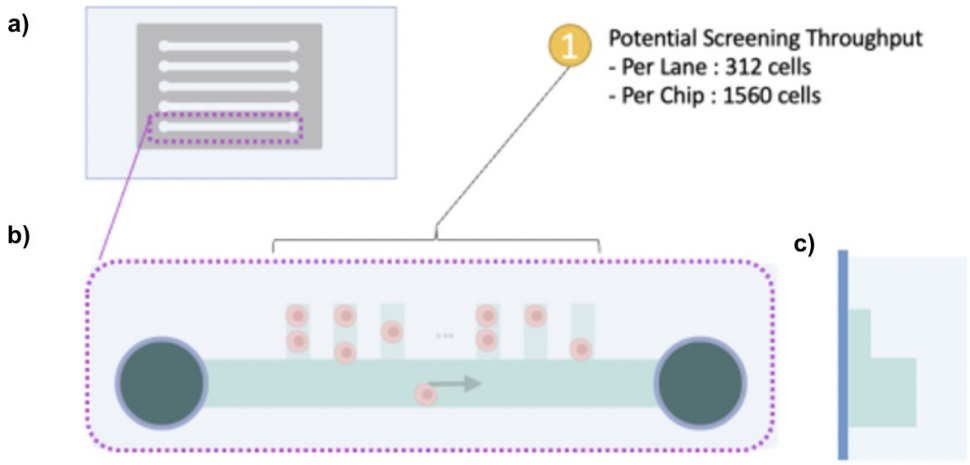

Figure 18 - A Jurkat mother machine
(a) Image depicting the top view of the device with 5 lanes. (b) Close of on the lane design showcasing a total of 312 trenches. (c) Side cross-section of a lane.

In this thesis, we introduce a microfluidic design for a mammalian mother machine that enables the imaging of Jurkat cells. The chip is composed of lanes providing continuous flow to 312 trenches that can host 3-6 cells each depending on their depth. Each device has 5 lanes for testing different conditions simultaneously, which makes its potential imaging throughput to 1500+ cells lineages per experiment. The geometry for the trenches was designed to accommodate typical Jurkat cells, which have been reported to have generally a diameter of 10 to 16 µm [45].

The manufacturing process of the microfluidic device was similar to the one for *E.coli* , which utilized both photolithography and soft lithography techniques. Initially, photolithography was utilized to generate a high-resolution master mold with precise microscale features using SU-8 photoresist and a silicon wafer. The wafer's initial design was inherited from Giselle McCallum and Krista Jager. I updated this design with improved alignment marks and an extra photoresist layer to construct channels with greater depths to mitigate clogging. Subsequently, the microfluidic chips were made from PDMS using the master wafer as a mold and bonded to a presterilized coverslip.

3.2.2. Development of a Microfluidics Set-up and Procedure

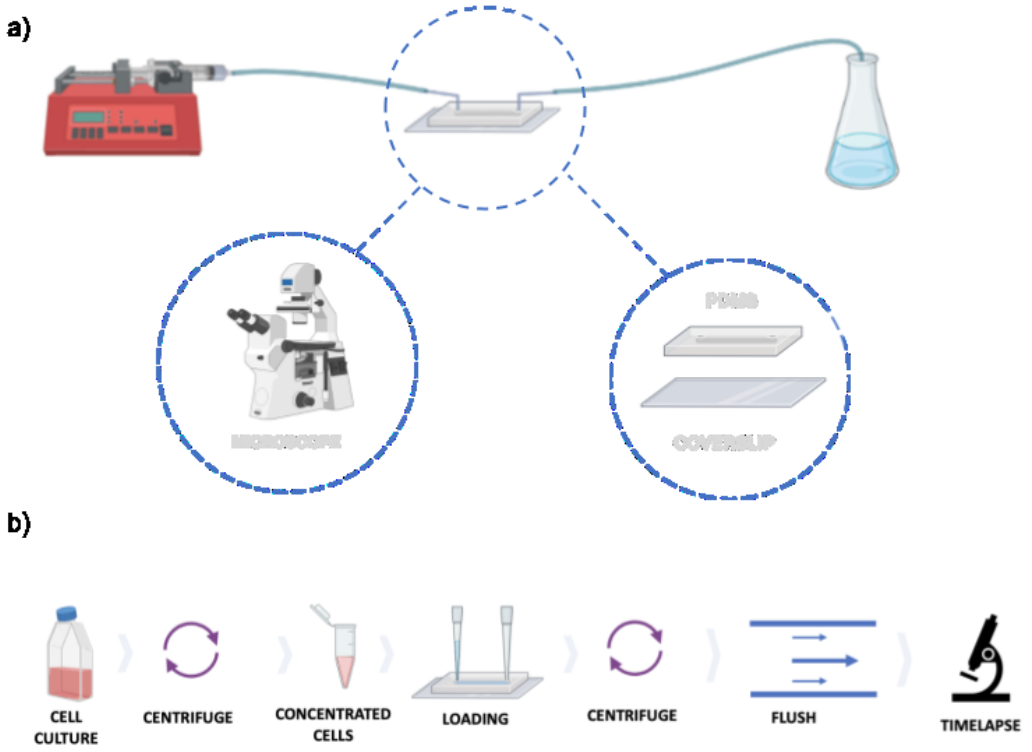

Figure 19 – Microfluidic set-up and experiment procedure
(a) Schematic of the set-up showcasing the device connected to a syringe pumps to providing continuous flow and to a flask collecting the waste. (b) Schematic of the loading protocol utilized in for experiments in this section.

The experimental setup consisted of syringe pumps, tubing, and tips connected to the microfluidic chip, ensuring a steady media flow for more than 24 hours. Time-lapse imaging was carried out using an inverted microscope equipped with a temperature-controlled incubation chamber. Although pH control was initially achieved through media buffers, a CO2 chamber was added to the setup towards the end of my masters for enhanced regulation. Prior to sample loading, the microfluidic chip and tubing were sterilized using isopropyl alcohol (IPA) and ultraviolet (UV) light, followed by a washing step with RPMI 1640. A concentrated cell suspension was then

introduced into the channels using a pipette within a biosafety cabinet, and the chip was centrifuged in a custom-made holder to ensure even distribution. Finally, the setup was completed by connecting the tubing, flushing cells at the inlets, and imaging the chips to assess the overall performance, paving the way for data collection and analysis.

3.3. RESULTS

3.3.1. Initial testing reveals viability and tracking challenges

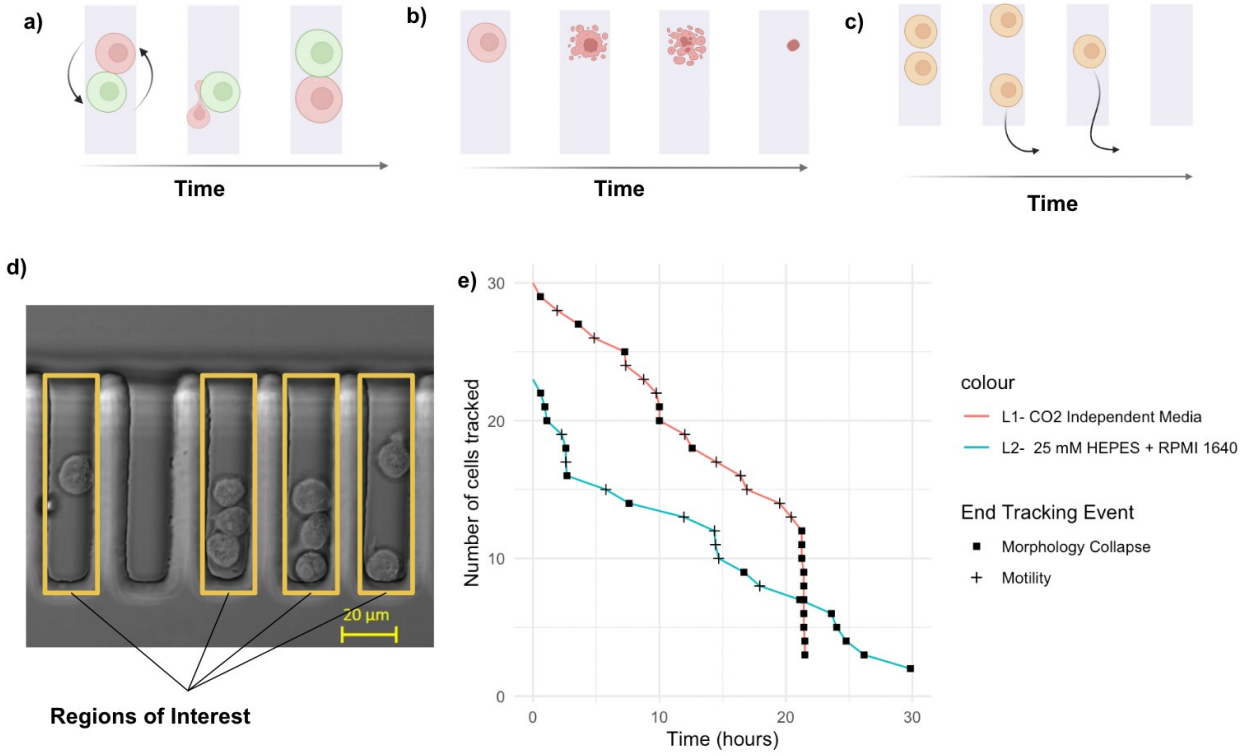

Figure 20 - Preliminary Challenges for a Jurkat mother machine
Images a to c showcase challenges identified through this assay. (a) Cells can swap location within trenches , (b) Cells morphology collapses over time, (c) Cells gain motility and migrate out of their trenches. (d) Image of cells in the microfluidic chip. Yellow rectangles represent the regions of interest, where cells were tracked to generate the graphic in €. € The graphic represents a sample of the number of cells manually tracked through time. Every time a cell leaves the region of interest or undergoes morphology collapse a cell is subtracted from the tracked population. Two pH regulation media buffers are tested, but it is not possible to conclude if one is better than the other one from this graph.

In this assay, we tested our experimental set-up and our ability to track cells. To accomplish this, we loaded two lanes of a microfluidic chip with a concentrated cell suspension. As our initial set-up lacked a CO2 chamber, we tested two different media conditions that could regulate pH with buffers. The first one was a CO2 Independent media (Gibco), which had previously been employed with Jurkat cells [46-47]. The second one was RPMI 1640 supplemented with 25 mM HEPES, which is a conventional pH-regulating buffer [48–50]. We chose a flow rate of 2.4 µL/h, which is comparable to [27] and the slowest our pumps could deliver. We then imaged four positions per lane, capturing sets of 11 trenches every 5 minutes for 30 hours.

From the time-lapse video, it became apparent that cells could change positions within a trench, which complicated the tracking of a "mother cell" (Fig. 20a). To address this, I considered each imaged trench as a region of interest and manually tracked phenotypes for all cells within the trench over time. Two primary phenotypes were identified as the causes for terminating cell tracking: increased motility and morphological collapse. The first one was observed when some cells become motile over time and eventually leave their respective trenches (Fig. 20b), which could be seen as a migration to a more favorable environment. The remaining cells within trenches ultimately exhibited morphological collapse and were considered dead (Fig. 20c). Tracking these phenotypes over time provided insights into the experiment's progression (Fig. 20d). For instance, the end trace for Lane 1 displayed a period where all remaining cells collapsed within a short amount of time. Upon further investigation this rapid death rate was attributed to a bubble that had flooded the channel moments before. Having said that, even before this bubble, cells seemed to be dying in both media conditions. One possible explanation was that Jurkat cells relied on one

another to provide growth factors that the media was lacking. This led us to explore other parameters that could be responsible for this like flow rate and adding conditioned media.

3.3.2. Flow conditions impact viability

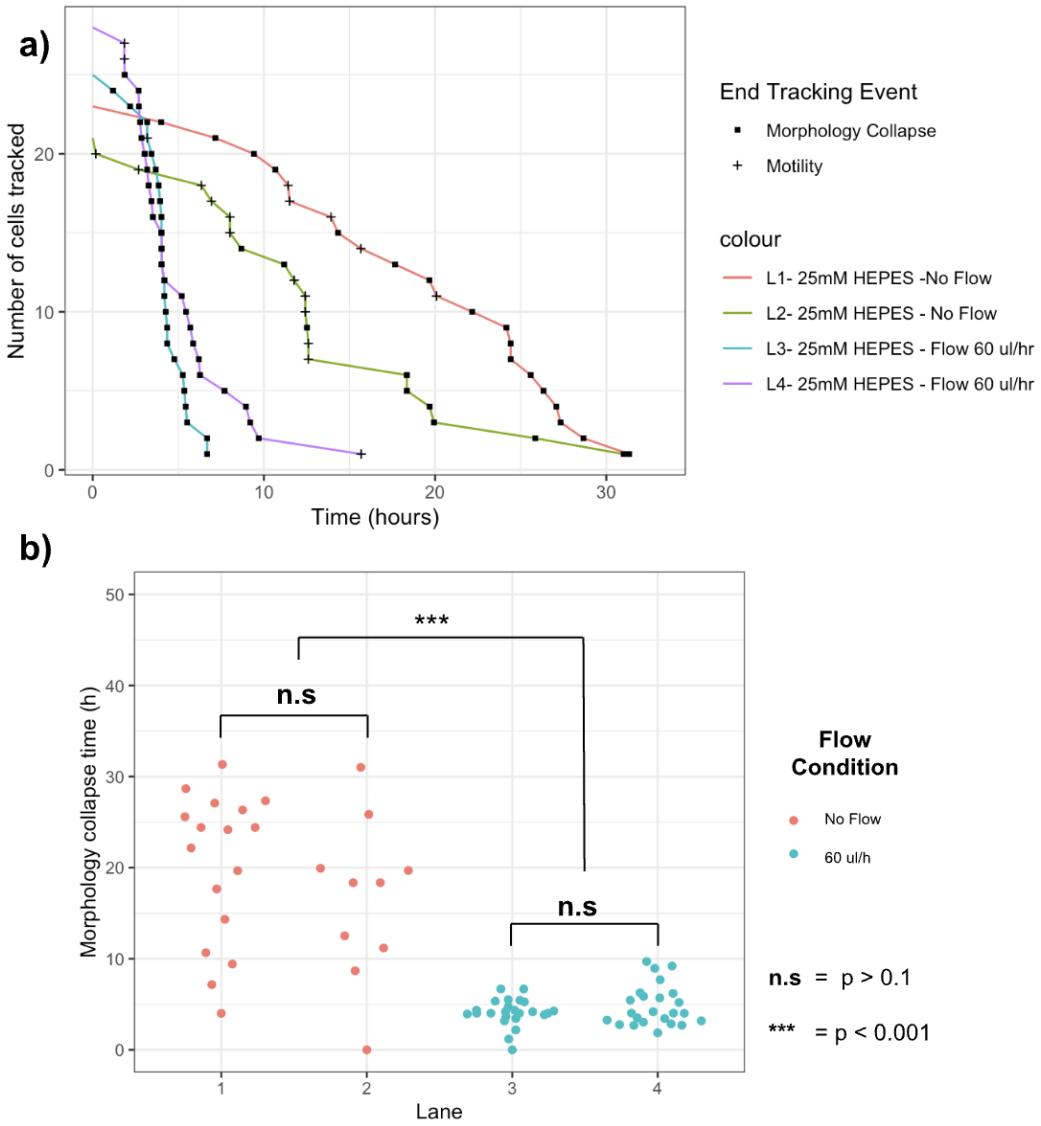

Figure 21 – Test for impact of flow conditions using 25mM HEPES as pH buffer
(a) Tracked sample population per lane overtime. Lanes 1 and 2 have no flow, lanes 3 and 4 have a flow rate of 60 µl/h. Lanes with flow appear to lose cells faster than the ones with flow. (b) This figure quantifies when cells lose their morphology.

In this experiment, we aimed to explore favorable flow conditions for hosting Jurkat cells in the mother machine for long-term time-lapse imaging. To investigate this, we tested two distinct

conditions in duplicate: two lanes with no flow and two lanes with a continuous flow of 60 µL/h. We decided to work exclusively with HEPES as our pH buffer to minimize the number of variables in this experiment. Based on a collaborator's suggestion, we used a 50% mixture of conditioned RPMI 1640 media to provide nutrients potentially lacking at low cell densities. As in section 3.3.1, we tracked cells in trenches at four positions per lane. Visualizing the number of tracked cells over time (Fig. 21a), it is possible to observe that lanes without flow keep their cells for longer. In fact, looking at morphology collapse times, it is possible to note that cells died significantly faster in flow conditions of 60 µL/h compared to no flow (Fig. 21b). This observation suggested that the flow either introduced an unfavorable component or removed a beneficial one. However, even in the absence of flow, cells appeared to die gradually, indicating that flow is not the sole contributor to reduced viability.

Various explanations can account for this phenomenon. One possible hypothesis is that light induced HEPES can become toxic for cells, as reported by Zigler *et al.* in [51]. Similarly, HEPES had been reported to work for a limited number of hours, so it is possible that at the microfluidic scale its ability to sustain the pH is diminished without flow. Cell contamination is also a challenge that is difficult to rule out completely from mammalian cell experiments, although the risk was mitigated with the use of penicillin and streptomycin in the media as well as a thorough cleaning of the chip with IPA and UV light. Nonetheless, these findings led us to upgrade our experimental setup with a CO2 chamber to circumvent issues related to HEPES and explore alternative flow conditions.

3.3.3. Upgraded set-up preliminary testing show improvement in viability

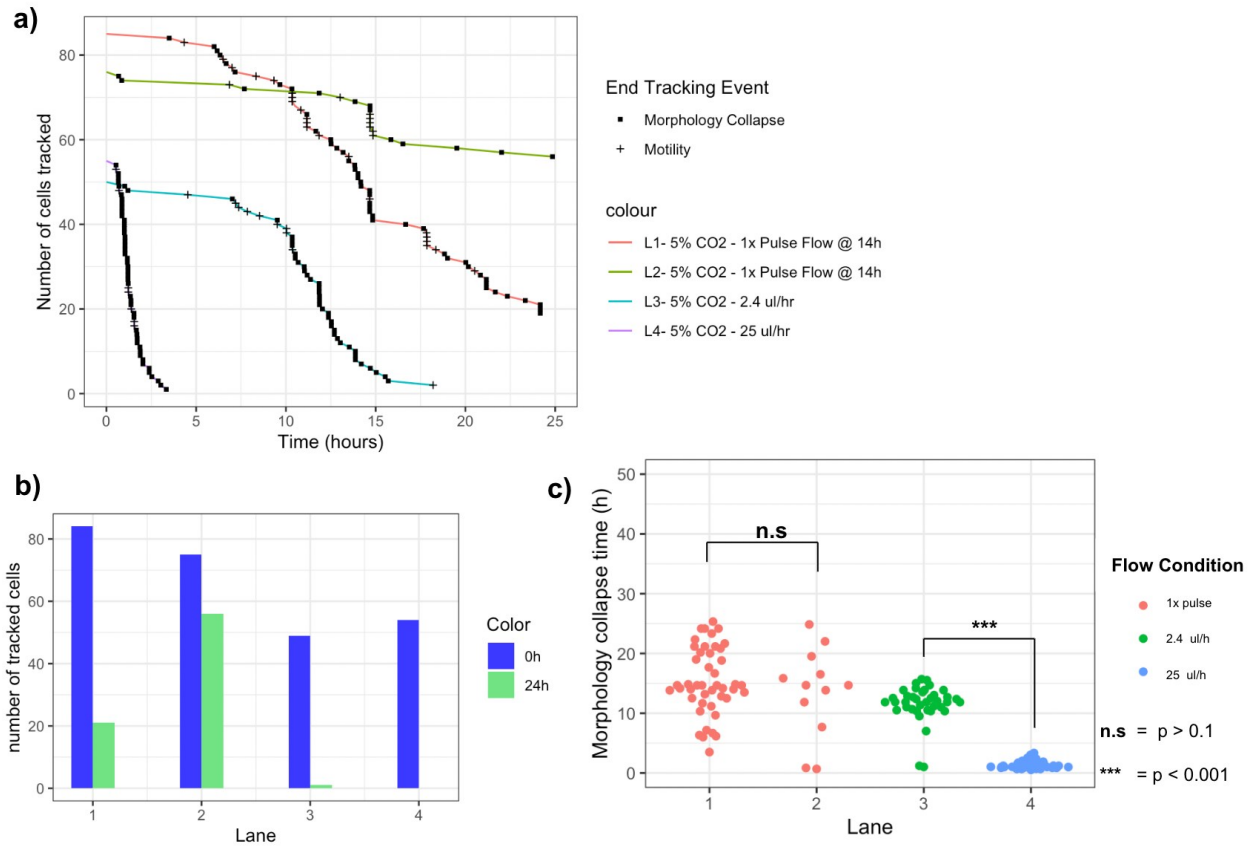

Figure 22 - Preliminary flow characterization with 5% CO2
(a) Tracked sample population for four lanes tested. Lanes 1 and 2 have no flow for most of the experiment except for 5 minutes at 14h15min, where a flow rate for 50 µl/h was used to replenish nutrient in the lane. Lanes 3 and 4 have flow rates of 2.4 µl/h and 25 µl/h respectively. (b) This graphic showcases the number of cells that are still in the region of interest and with their morphology viable at the start of the experiment and after 24h. (c) This graphic quantifies the time cells lose their morphology.

In this final experiment, I aimed to evaluate our upgraded experimental setup, which now included a CO2 chamber set at 5%. Similarly, I wanted to explore various flows to guide the next student in determining the optimal conditions for hosting Jurkat cells in our device. To achieve this, I loaded four lanes with a Jurkat cell suspension, each with a unique flow condition. Lanes 1 and 2 had no flow for the majority of the experiment, with a brief 5 min exception at 14h, when

we circulated media at 50 μL/min to replenish nutrients. Lanes 3 and 4 had continuous flows of 2.5 μL/h and 25 μL/h, respectively.

Our observations revealed that lanes without flow performed statistically better than those with flow (Fig. 22c). Lane 2 seemed to provide the most favorable conditions, maintaining the majority of cells past 24 h (Fig. 22b). Although Lane 1 had similar conditions to Lane 2, fewer cells made it after 24h, which might be due to lane-to-lane variability and warrants further investigation. Similarly, it was observed that higher flow rate the faster cell's morphology collapse. This could point to the hypothesis that flow removes a beneficial component for cells that is emphasized the faster the flow is. In fact, it is possible that our Jurkat cell line produces little to no Interleukin-2 (IL-2) (lymphokine that promotes cell proliferation) [52], which could explain cells being more vulnerable at low densities. Nonetheless, these findings serve as a baseline to direct future experiments to further characterize optimal working conditions for adapting the mother machine to Jurkat cells.

3.4. Next steps to troubleshoot and Future work.

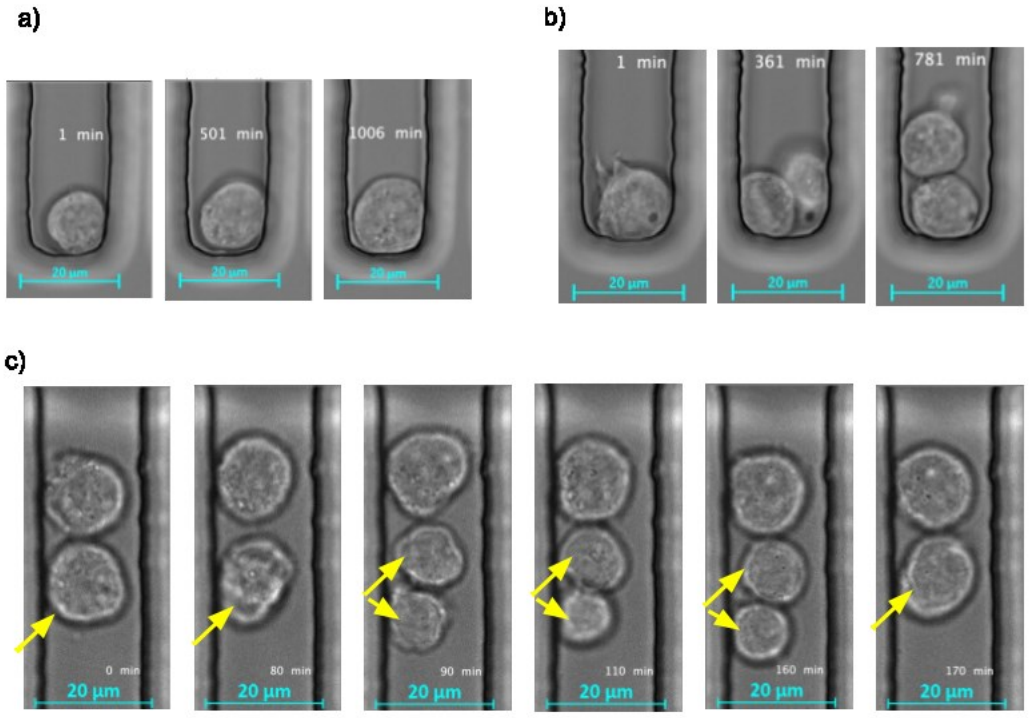

Figure 23 – Phenotypes that could be further explored in future experiments.
(a) Cell growth, (b) Cell division and other rare phenotypes like (c) cells remerging after mitosis.

Although this project did not implement a complete version of the mother machine for Jurkat cells, it established a baseline and identified key issues to solve. Likewise, it allowed us to observe interesting phenotypes such as growth (Fig. 23a), mitosis (Fig. 23b) and cell remerging events (Fig. 23c). Nonetheless, the best iteration and conditions explored are arguably found in Lane 2 of the last assay (Section 3.3.3), which hosted 74% of cells for at least 24 h using a 5% CO2 chamber without flow. Next steps should aim to further characterize this condition with replicates and understand the lane-to-lane variability aspects. Similarly, it would be interesting to explore other additives to the media such as IL-2 and/or Sodium Pyruvate, which was used in the mammalian mother machine publication [23] and it has been suggested as additive to Jurkats at

low densities [53]. Additionally, using a Jurkat cell line that expresses a fluorescence protein constitutively would be a good improvement, as it opens the door to use segmentation methods and can be used to determine the death of a cell more accurately.

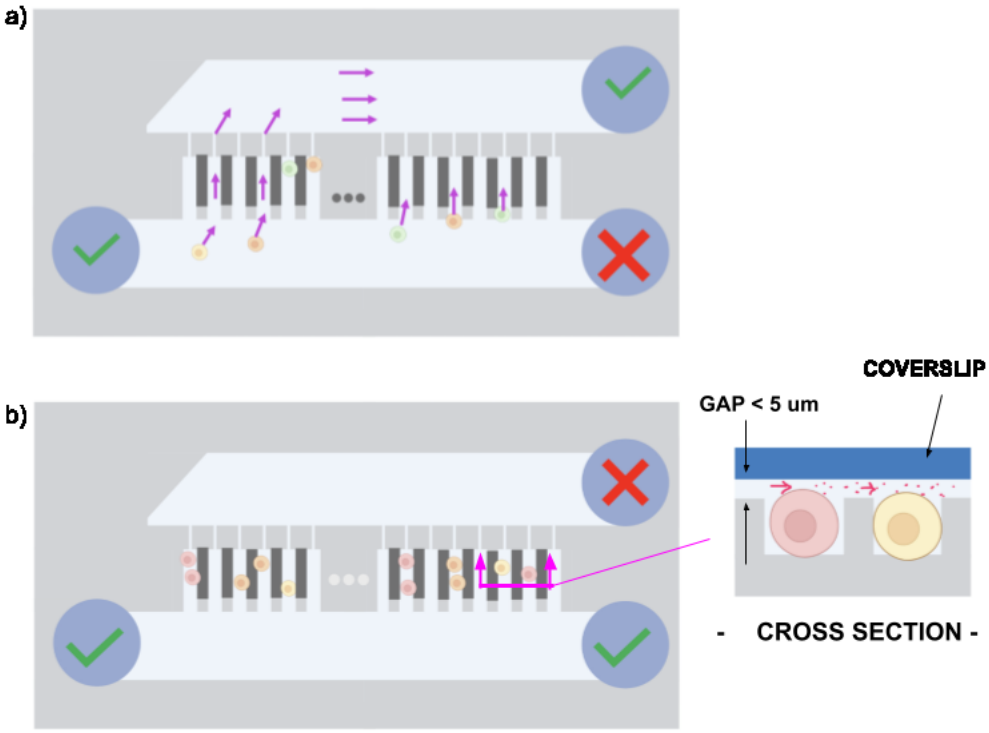

Figure 24 – New microfluidic device for future testing
Two upgrades are presented in this figure, (a) shows a more controlled method using flow with an additional outlet located behind trenches (b) presents a gap between the trench geometry and the coverslip to provide better access to leaked growth factors from neighbouring cells.

Future work can look at exploring design modifications to reduce loading stress and improve cell to cell nutrient dispersion. Figure 11 proposes design alterations to achieve this. The first modification (Fig. 11a) would be to add a small opening at the end of trenches along with a back channel. This would allow the user to explore other loading methods, such as gravity loading or passive flow loading, which would likely reduce the stress on cells and improve their long-term viability. Likewise, it gives a means to control a flow that pushes cells into their traps, which could be used at low flow rates to prevent cells leaving their trenches. The second proposed change is

to connect trenches with a small gap (Fig. 11b), which would allow nutrients to leak across trenches and likely increase viability.

CHAPTER 4

Conclusion

4.1. Conclusion of our work with *E.coli*

In brief, this thesis successfully addressed its primary objective by implementing the necessary equipment for executing the existing *E.coli* screening technique called Single Cell Isolation Following Time Lapse (SIFT) [22]. More specifically, this work established a manufacturing protocol for the microfluidic device. It showcased the chip capabilities for high-throughput screening by imaging a mock-up *E.coli* population and tracking the constitutive expression of a fluorescent protein for 418 monoclonal lineages for an average of 32 generations. This was made possible with the use of an existing segmentation code called Deep Learning for Time-lapse Analysis (DeLTA) [41]. Similarly, this work successfully implemented a pressure system to control push-down valves in the microfluidic device, which were tested to achieve full closure between 30-40 psi. Additionally, this project accomplished the design, build and testing of optical tweezers, which combined with the presented microfluidic device allows the user to manipulate a single cell after timelapse and isolate it from the population. A proof-of-concept mock-up assay successfully demonstrated the isolation and expansion of three cells expressing CFP from a mixed population consisting of 98% of cells expressing RFP and only 2% of cells expressing CFP. Finally, in collaboration with Paige Allard, this work successfully phenotyped a pooled library of *E.coli* cells with synthetic gene oscillators. However, existing challenges from the method prevented us from isolating single cells, which highlights the need for optimized loading protocols, anti-biofilm strategies and a more flexible iteration of the

segmentation code. Nonetheless, by combining a high-throughput microfluidic device with optical tweezers, this approach paves the way for screening time-varying genetic circuits in mixed populations of *E.coli* , while enabling the accurate isolation of individual cells for further analysis.

4.2. Conclusion of our work in Jurkat cells

Moreover, this thesis partially addressed its secondary objective, which consisted of adapting the mother machine to Jurkat cells. To this end, this work introduced a design for a mammalian mother machine as well as a protocol for its manufacture. Its capabilities were initially tested in an environment without 5% CO2, but with media buffers to compensate for this. Preliminary results indicated challenges currently not encountered with the *E.coli* device including: cells swapping positions within trenches, cells gaining motility overtime and leaving trenches and viability issues observed through cells' morphology collapsing. Focusing our research on the latter issue, timelapse tracking of multiple lanes in the device suggests that stagnant flow conditions are more favorable for our cells compared to a 60 µL/hr flow rate of 50% conditioned media with 25mM HEPES serving as a pH regulator in RPMI 1640. In fact, a subsequent experiment with an upgraded set-up including a CO2 chamber showcased the most promising condition tested with a semi stagnant flow (1 pulse of flow at 50 µL/h for x min at 14h in the experiment) for which 74 % of the cells are deemed viable for more than 24h. Our working hypothesis is that flow possibly removes a favorable component for Jurkat cells like IL-2 or other growth factors, which could be explored further in future studies. Next steps should aim at further characterizing the most promising condition tested with replicates so as to understand lane to lane variability. Lastly, this thesis presented a potential new design for the mother machine to test a different loading method and a geometry that provides cells in trenches with better access to

leaked growth factors from their neighbors. Nevertheless, these preliminary results can serve as a foundation for future researchers seeking to develop a Jurkat mother machine.

4.3. Significance for the field and broader applications

Our research demonstrates the replicability of the SIFT technique, providing a powerful tool for tracking gene expression in *E.coli* populations with single-cell resolution across multiple generations. This has significant implications for various fields, including the study of time-varying phenotypes and the development of new synthetic biological circuits. By allowing the characterization of multiple replicates and variations of genetic circuits, our microfluidic platform enhances our understanding of population variability and underlying mechanisms. The integration of optical tweezers further enables cell manipulation and the extraction of specific cells for additional characterization and optimization. The applicability of this technique extends beyond simple gene oscillators, potentially contributing to the development of analog gene circuits, counters, and biological control systems. Moreover, its use in prokaryote research opens avenues for creating novel probiotics and thorough characterization of their properties. Overall, our research contributes to the advancement of synthetic biology, offering new possibilities for future investigation and application.

Expanding this technique to mammalian cells offers a valuable platform for understanding gene expression levels within suspension cells over time and under various environmental conditions. This capability has significant potential in the development of new immunotherapies, such as investigating the impact of specific Chimeric Antigen Receptors (CARs) on cells. By tracking cell division times in response to a particular CAR, researchers can gain insights into the

burden imposed by the genetic edit on the cells. Overall, the adaptation of this technique for mammalian cells could enhance our understanding of gene expression dynamics for suspension cells and pave the way for innovative therapeutic approaches.

4.4. Last words

In conclusion, our research presents a powerful tool to study and develop novel biological circuits for *E.coli* and lays a foundation to expand this work for mammalian suspension cells. As such, this work can serve as a step forward in the development of technologies to catalyze discoveries and innovation for synthetic biology.

CHAPTER 5

Materials and Methods

5.1. PART 1 - Experiments with *E.coli*

5.1.1. Photolithography

To fabricate the molds, we used 4 inches silicon wafers from University Wafers. All wafers were fabricated in a class 100 cleanroom at Mcgill's Nanotools facilities (Montreal, Canada). The following sections describe the photolithography recipes for the wafers in this work.

5.1.1.1. Photolithography Recipes for *E.coli* Microfluidic Devices

The *E.coli* mother machine for SIFT is a multilayer device, thus it requires two wafers for its fabrication. The first wafer is for the trenches, lanes and valves structures. The second wafer is for air channels to control the valves.

Wafer 1 - Layer 1: Trenches

The wafer was initially cleaned with Acetone/IPA/DI for approximately 30 sec each. It was then dehydrated for 15 min at 150 °C in a hotplate. The first layer coated was SU-8 2001(Kayaku), which was done in two steps of 500/87/10 and 950/348/60 **(speed/acceleration**

/seconds) using a Laurell spin coater (WS-400-6NPP-LITE). Then it was soft baked respectively at 65°C for 1 min, 95 °C for 1 min and 20 sec and 65 °C for 1 min. Following this, the wafer was exposed to the "trench" mask (Quartz-Toppman) using a mask aligner (EVG-620) for constant exposure at 120 mJ/cm^2. It was then post baked at 65°C for 1 min, 95 °C for 1 min 30 sec and 65 °C for 1 min. The wafer was then submerged in SU-8 developer for 1 min 40 sec in a dish followed by a 20 sec rinse using fresh developer. Then it was immersed and rinsed with IPA and DI respectively. The wafer was hard baked at 150 °C for 15 min. To validate the height of the layer, the wafer was probed at 3 locations using a profiler (Ambios XP200). The measured height of this layer was between 1.23 µm and 1.42 µm.

Wafer 1 - Layer 2: Lanes

The second layer was spin coated with SU-8 2015 (Kayaku) in two steps of 500/87/10 and 1500/348/60. Then it was soft baked respectively at 65°C for 1 min, 95 °C for 3.5 min and 65 °C for 1 min. The alignment marks were cleaned using pure SU-8 developer in droplets with a swab. Following this, layer 1 on the wafer was aligned with the "lanes" mask (CAD Art) and exposed at 180 mJ/cm^3. It was then post baked at 65°C for 1 min, 95 °C for 4 min and 65 °C for 1 min. The wafer was then immersed in SU-8 developer for 1 min 40 sec in a dish and rinsed for 20 sec using fresh developer from the bottle. Then it was submerged and rinsed with IPA and DI water respectively. The wafer was hard baked at 150 °C for 15 min and the height of this layer was measured between 21.3 µm and 22.3 µm.

Wafer 1 - Layer 3: Valves

The third layer was spin coated with AZ-10XT (Kayaku) at speeds of 500/87/10 and 1370/348/30 respectively. Then it was soft baked at 110°C for 3 min and left on the bench for 40 min at ambient temperature. The alignment marks were cleaned with droplets of pure AZ-400K developer using a swab. Following this, the wafer was aligned with the "valves" mask (CADArt) and exposed at 1275 mJ/cm^3. The wafer was then submerged in AZ-400K developer diluted 1:3 in DI water using a dish for approximately 3 min. It was rinsed with a bottle of fresh DI water for about 30 sec. Then the wafer was hard baked (thermal reflow) at 130 °C for 5 min. The features in this layer were rounded so the height was determined at the max peak which was measured between 19.26 μm and 22.3 μm.

Wafer 2 - Layer 1: Air Channels

The second mold referred to as the air control wafer was fabricated in a similar manner. The cleaning and dehydration process were the same as the first one. This wafer had only one layer spin coated with SU-8 2050 at speed of 500/87/10 and 1750/348/60 respectively. Soft baking occurred at 65°C for 3 min, 95 °C for 9 min and 65 °C for 1 min. Following this, the layer was exposed to the "air valves" mask at 245 mJ/cm^3. It was then post baked at 65°C for 2 min, 95 °C for 7 min and 65 °C for 1 min. The wafer was developed in SU-8 developer for 5 min in a dish and rinsed using fresh developer from the bottle. Then it was immersed and rinsed in IPA and DI water respectively. The wafer was hard baked at 150 °C for 15 min. The measured height of this layer was between 59.18 μm and 63.6 μm.

5.1.2. Soft Lithography

5.1.2.1. Soft Lithography Recipe for *E.coli* Devices

This procedure was based on worked performed by Luro et.al in [22]. The device for SIFT was fabricated in two layers of PDMS (Sylgard 184 Silicone Elastomer). The first mold was spin coated on the trenches wafer at a ratio of 20:1 (monomer : curing agent) and a speed of 1250 for 45 seconds (Laurell Model WS-650MZ-8NPPB) to target a thickness of 70 μm[22]. The second mold was poured on the air control wafer at a ratio of 5:1. Both slabs were degassed in a desiccator for 45 min and baked in an oven at 65 °C for 90 min the trenches mold and 45 min the air control. Two chips from the air control mold were excised, punched with a 0.75 mm biopsy puncher (World Precision Instruments) and cleaned with Scotch tape. The cured trenches wafer and air control chips were exposed to plasma at an oxygen flow rate of 45 sccm with a power of 30W for 15 seconds. The chips were then aligned using DI water droplets in between layers and evaporated in a hotplate at 45 °C for 1.5h to complete the bonding. Two chips were excised from the new wafer and inlets/outlets were punched with a 0.75 mm biopsy puncher. They were then sonicated for 20 min in IPA and dried in an oven at 65 °C for 15 min. Glass coverslips (Fisher Scientific: 22x40 mm #1.5) were cleaned with potassium hydroxide, air blown and dried for 20 min at 65 °C in an oven. The PDMS chips were bonded to coverslips by plasma cleaning with the same recipe as the chip to wafer bond. They were then baked 100°C for 10 min in a hotplate, then at 65 °C for 30 min in an oven and left at ambient temperature for at least 2h.

5.1.3. Pressure Set-up for *E.coli* Experiments

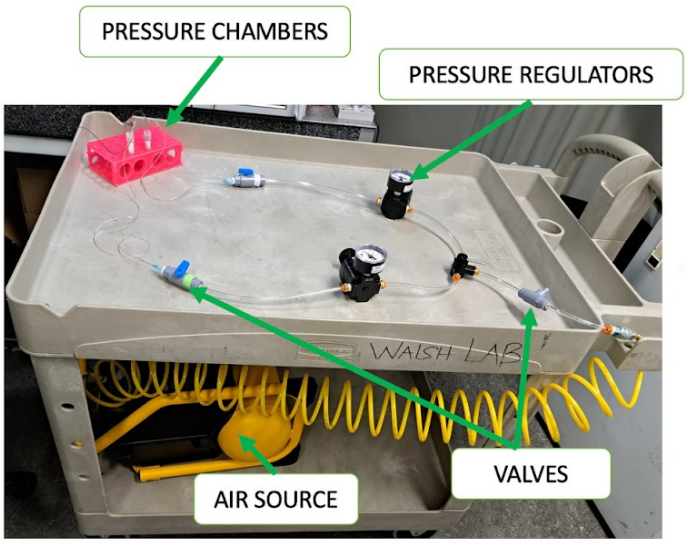

Figure 25 – Pressure Set-up for operating SIFT

The pressure set-up was responsible for bringing compressed air into the system to control valves in the *E.coli* chips. Similar set-ups generally use pressure from the building [22, 54], but this option was not available for us. In fact, we wanted a portable set-up that could keep valves closed even while transporting the chip so we chose to use an air compressor as a pressure source (DEWALT D55140 - Home Depot) . The pressurized air from the compressor was split into two flows with a diverting valve (45695K32 - Mmcaster Carr), three shut-off valves (4757K21 – Mmcaster Carr), tubing (5648K611- Mmcaster Carr) and adapters (5111K82/6534K56/ 51525K437 - Mmcaster Carr). The pressure control was done manually with precision air regulators (6162K22 - Mmcaster Carr) and dial gauges (4000K563 - Mmcaster Carr). Similarly,

liquid pressure chambers were made using cryovials (10018-756 - VWR) with holes for tubing and sealed with epoxy (4200602 - Gorilla) as inspired by [38]. The connection to the chip was made with syringe tips (75165A678 - Mcmaster Carr) and Tygon tubing (89404-302 - VWR).

5.1.4. Optical Set-up for *E.coli* Experiments

The set-up of the optical trap was based on work from Luro [22] with details defined by me. Most of the external optomechanical parts were mounted on a rail (RC1 - Thorlabs) to constrain motion and simplify assembly. The laser used was a 1,064 nm ytterbium (IPG Photonics YLR-10-1064-LP) in continuous wave mode with a beam diameter of approximately 5 mm. The laser was generally operated around 20% of its total power which represents ~2 W. However, most of this power was directed to a beam block (LB2 - Thorlabs) using a rotating half-wave followed by a polarizing beam splitter (Thorlabs VBA05-1064). For safety purposes, a laser shutter (Thorlabs SHB1T) was installed after the beam splitter to toggle the optical tweezers on and off. The beam diameter was increased 2X using an achromatic beam expander (Thorlabs GBE02-C) and guided to a higher plane using a custom periscope made from two aluminum mirrors (PF10-03-G01 - Thorlabs) , 45° adapters (H45 - Thorlabs) and kinematic mounts (KS1 - Thorlabs). The laser was then guided through a 1:1 Keplerian telescope made from two convex lenses (Thorlabs LA1131-C). The beam was then passed through the epi-illumination port of a Zeiss Axio Observer 7 microscope, integrated with a 1064nm mirror (RAPP) to reflect it towards a 100X APO oil objective with an NA of 1.49 (MRD01991 - Nikon). The NIR beam was filtered (Chroma ET750sp-2p8) before reaching an Orca Flash 4.0 LT camera (Hamamatsu). The alignment of the optical tweezers was achieved following guidelines in [39]. It was helpful to have a collinear visible red guide beam that came with the IPG laser as well as a coarse alignment camera (14-675 - edmund optics). The mirror on the periscope served as a steering mechanism for the laser. Similarly, the distance between the telescope lenses allowed us to move the optical trap in

the z direction. Cell trapping was generally achieved with a laser output of 2W and attenuated to 100 - 200 mW before entering the microscope.

5.1.5. *E.coli* Cell Preparation

The cell culture protocol was done with the help of Paige Allard, who provided the constructed strains and helped me prepare them for loading. For the red and blue assay, two strains were used: **PA12** who expresses mCherry continuously and **LPT35** who expresses CFP endogenously. As the strains were available to us frozen, we only needed to grow an overnight culture of each in 5 mL of LB in an incubator shaker at 37°C and 200 rpm. The day of the experiment, both cultures were diluted 1:100 in 5 ml of imaging media (M9 salts, 0.2% (w/v) glucose, 1 mM MgSO4, 0.1 mM CaCl2, 20μg/mL uracil, 0.2 g/L casamino acids and 0.85 g/L Pluronic F-108 (Sigma Aldrich)) and placed to grow in the shaker again for 1.5 h. Lastly, a new 5 ml culture was made from both tubes at a ratio of 2% CFP and 98% RFP, which was left on the bench for 30 min before running the loading protocol. Similarly, for the oscillator experiments, a library of plasmids was generated starting from plasmid *pSL229* gifted by Dr. Luro and isolated in [22]. Then they were mutated via error prone polymerase chain reaction (PCR). The library was then transfected on MG1655 strains and plated on an agar pad. Colonies from the plate were scraped into 5 mL of imaging media and grown for 1.5h at 37°C in a shaker at 200 rpm. Following this, they were left on the bench for 30 min prior executing the loading protocol.

5.1.6. Microfluidic set-up for *E.coli* Experiments

All liquid connections were made with Tygon tubing (89404-302 - VWR) and syringe tips (75165A685 - Mcmaster Carr). Autoclaved 20mL syringes (14-823-16J - Fisher Scientific) were

used for all liquid handling with *E.coli* microfluidics. The bonding of valves was tested with food colorant in DI water prior to all experiments by gradually increasing pressure and achieving full closure of valves at around 30-35 psi. Lanes were pre-wetted with bovine serum albumin (BSA) using gel tips to prevent biofilm build-up. Prior loading, a 5 ml culture of cells was concentrated by centrifugation at 3000 g for at least 40 sec followed by the removal of supernatant. The mixture was then pipetted into outlets of growth channels with valves in-between lanes closed to guide the flow at the right location. The following steps differed based on three loading strategies explored: diffusion, centrifugation and lane drying. The diffusion method, originally used in[22], consisted in closing the side valves to turn the growth lane into an isolated chamber for at least 60 min to increase the probability that cells get trapped in trenches and load the chip. The centrifugation method was the typical loading process for mother machine chips which consisted of spinning the loaded chip at 5000g for 10 min in a centrifuge and forcing cells into position. The lane drying method involved leaving the inlets and outlets exposed to air for at least 2h after pipetting in the culture to dry the lane, make cells smaller and force them to go in trenches which was the only place left with media. Following loading, growth lanes were generally fed with imaging media at a flow rate of 5-10 μL/min with syringe pumps (New Era Pump System) for the duration of the experiment.

5.1.7. Microfluidic Cleaning Strategies for *E.coli*

A cleaning procedure was developed to mitigate biofilm build up at the inlet and prevent cells floating in the growth lane at the time of trapping. It was generally done during loading by diffusion or when all valves were closed and the cleaning outlet port located next to the inlet was unclamped to allow flow Fig(x). In brief, a solution of 10% bleach diluted in DI water was flown at 50 µL/min for 15 min, followed by 10% ethanol diluted in DI water at 50 µL/min for 20 min, and then imaging media for 20 min at 50 µL/min. These manipulations were facilitated using Y junctions (Amazon) and tube clamps (Amazon). In a similar manner, prior to trapping cells, the isolation lane was pre-sterilized with a cleaning protocol to ensure only the desired cell was captured at the outlet. The cleaning was executed while keeping the in between lane valves closed until cell isolation. The method involved flowing a solution of 10% bleach diluted in DI water at 50 µL/min for 45 min, followed by 10% ethanol diluted in DI water at 50 µL/min for 30 min, and then imaging media for 15 min at 50 µL/min.

5.1.8. Cell Imaging Protocol for *E.coli*

Timelapse for experiments was done using a Zeiss Axio Observer inverted microscope with a 63x Plan-Apochromat M27 oil objective (NA 1.40), an Orca Flash 4.0 LT camera (Hamamatsu), and an LED epifluorescence illuminator (Collibri 7). The microscope was equipped with a temperature-controlled incubation chamber set at 37 °C. The duration and interval depended on

assay carried out. For the blue and red assay, the duration was at least 12 h at (5/8) min every frame. For the dual feedback oscillator experiments the duration was at least 12 h at 8 min every frame. Although the device was equipped with four sets of growth and isolation lanes, given the complexity of the set-up, I chose to work with only one of those sets.

5.1.9. Cell Segmentation Protocol and Analysis for *E.coli* Experiments

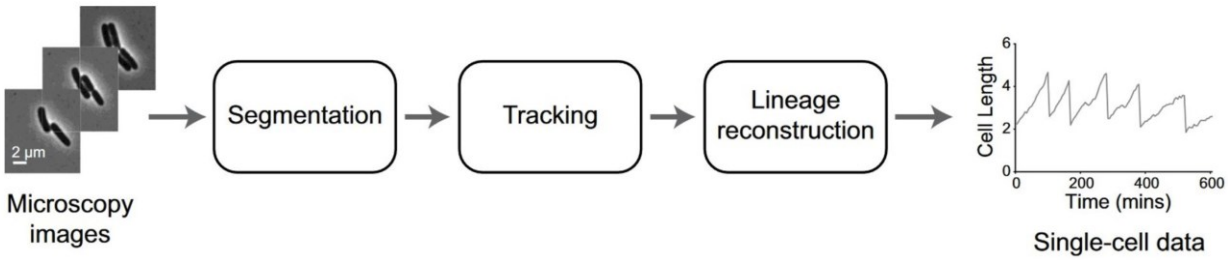

Figure 26 - DeLTA (Deep Learning for Time-lapse Analysis)

The time-lapse images were processed using a deep learning-based program called Deep Learning for Time-lapse Analysis (DeLTA) [41]. It should be noted that the code was implemented by Hans Olischlager and tested through this project. DeLTA was developed to segment cells from a timelapse using a U-net architecture. In our iteration of this code, it was trained on *in silico* modeled mother machine experiments generated with the help of Euan Joly-Smith. The way it was used in this thesis was to take CZI files from mother machine experiments as input and executing an iteration DeLTA through a Jupyter notebook. The deep learning aspect was primarily used to segment to identify the outline of cells with an emphasis on border pixels. It should be noted that the identification of regions of interests (trenches) and the tracking of cell lineages was performed with complementary code developed by Hans Olischlager, Euan Joly-Smith and Dr. Laurent Potvin-Trottier.

Upon execution of this segmentation pipeline, a MATLAB file was generated containing important parameters such as cell area, mean fluorescence, position, and trench ID. I developed a code that wrangles this output so that it can be integrated into our existing analysis pipeline, which comprises several MATLAB functions. With this pipeline, we can perform basic operations such as purging empty trenches and generating time traces for critical parameters like area, fluorescence, and doubling time. Due to the nature of our work, to execute the SIFT technique, a rapid segmentation is required such that it can be done while the experiment is still running on the microscope, which presented a challenge and can be further optimized.

5.1.10. Cell Isolation Protocol for *E.coli* Experiments

Cells of interest were generally identified through segmentation or by looking at the time lapse of a position. Prior trapping, the media fed in the growth lane was swapped to a minimal nutrients' version (imaging media with glucose replaced by glycerol) at 5 µL/min for at least 1h. This reduced the size of cells and made them easier to trap. Trapping was achieved with the inlet/outlet valves closed to stop the flow and only for a brief moment the in-between lane valves were open to move the cell in the isolation lane. The isolation of *E.coli* cells was performed with the laser focal point aimed directly at a cell and the XYZ stage of the microscope moved the microfluidic chip to position the cell in the isolation lane. The desired cell was then recovered by stopping the laser, closing the in-between lane valves, opening the inlet valves , and flowing imaging media at 50 µL/min for 3 min with the ~5 cm tubing outlet directed at the well of a 96 well plate. Lastly, the content of the well was left to incubate overnight at 37 °C.

5.2. PART 2 - Experiments with Jurkat cells

5.2.1. Mask Design for Jurkat Devices

The mask design was inherited from Giselle McCallum and updated with a channel height bigger to help mitigate clogging issues. Through this work, we also develop a new array with a potential SIFT design for mammalian cells, but it was left at the concept stage as we focused on the simple version.

5.2.2. Photolithography Recipes for Jurkat Microfluidic Devices

Wafer 3 - Layer 1: Trenches

A 4 inch silicon wafer was cleaned and dehydrated just like the *E.coli* ones. The wafer was plasma cleaned at 100 W for 5 min using a DSB6000 Oxygen Asher. One layer of SU-8 2015 was spin coated at 500/87/10 and 1500/348/60 respectively (speed/acceleration/seconds) . The soft baking happened at 65°C for 1 min, 95 °C for 3.5 min and 65 °C for 1 min. The wafer was exposed to the "mammalian trench" mask (CADArt) at 180 mJ/cm^3. It was then post baked at 65°C for 1 min, 95 °C for 4 min and 65 °C for 1 min. The wafer was immersed in SU-8 developer for 1 min 40 sec in a dish and rinsed using fresh developer for 20 sec. It was then submerged and rinsed in IPA and DI water respectively. The wafer hard baking happened at 150 °C for 15 min. The measured height of this layer was between 20.5 μm and 20.9 μm.

Wafer 3 - Layer 2: Lane Padding

A layer of SU-8 2050 was spin coated at 500/87/10 and 1750/348/60 respectively. Soft baked at 65°C for 3 min, 95 °C for 9 min and 65 °C for 1 min. The wafer was exposed to the "padding" mask (CADArt) at 215 mJ/cm^3. The post baking occurred at 65°C for 2 min, 95 °C for 7 min and 65 °C for 1 min. The wafer was then immersed in SU-8 developer for 7 min in a dish and rinsed with fresh developer for 20 sec. Then it was submerged and rinsed in IPA and DI water respectively. Lastly, the wafer was hard baked at 150 °C for 15 min. The measured height of this layer was between 48 and 50.5 μm.

5.2.3. Fabrication of the microfluidic device for Jurkat cells

The mammalian mother machine is made of a single layer PDMS slab poured at a ratio of 10:1 (40g:4g) on the wafer. The slab was desiccated for ~45 min and baked at 65°C for 90 min in an oven. Two chips were excised from the array, inlets/outlets were made using a 0.75 mm biopsy puncher and cleaned with tape. They were then sonicated for 20 min in IPA, dried at 65 °C in an oven for 15 min. Glass coverslips were cleaned like for the *E.coli* device and bonded on with the microfluidic chips using the same plasma cleaning parameters as above. The chips were then baked 100°C for 10 min in a hotplate, then at 65 °C for 30 min in an oven and left at ambient temperature for at least 2h.

5.2.4. Experimental Microfluidic Set-up

The tubing, syringe tips and pumps used were the same specifications as in the *E.coli* experiments. The tubing and syringe tips used for the mammalian mother machine were sterilized in an autoclave. The PDMS chip, tubing and syringes were also placed under UV light for at least 30 min in a biosafety cabinet. They were then cleaned with 70% Ethanol, autoclaved DI water and flush with RPMI (Corning) or CO2 independent media (Thermo Fisher) depending on the assay. Sterile syringes were prepared with various combinations of media to explore the optimal

conditions for Jurkats in the device (see Table 1). In a biosafety cabinet, lanes in the device were pre-wetted with RPMI using gel tips. A culture of 10 ml Jurkat cells was concentrated to ~ 100 ul by centrifugation at 300g. The culture was pipetted into the PDMS chip and spun at 200g for 5 min. The tubing was connected, and media was flown to flush the inlets. The temperature control around the device was achieved using the incubator from the microscope at 37°C.

Table 1 - Media combinations tested.

SECTION	**MEDIA**
3.5	RPMI 1640 + 25mM HEPES & CO2 Independent Media
3.6	RPMI 1640 + 50% Conditioned media + 25mM HEPES + 1u Penstresp
3.7	RPMI 1640 + 50% Conditioned media + 1u Penstrep

5.2.5. Cell Imaging Protocol for Jurkat Experiments

Timelapse for experiments with Jurkat cells were done also with the same microscope as the *E.coli* experiments. They were imaged at 40X Plan-Apochromat M27 (NA 0.95) or at 60X Plan-Apochromat M27 oil objective (NA 1.40), on brightfield every 10 min for at least 24 hours. The mammalian mother machine developed here was in its early prototypes, so we did not explore automated methods of segmenting cells. Generally, experiments were carried out imaging 4 or 5 lanes in the device.

5.2.6. Data Analysis for Jurkat Experiments

In this analysis, four positions per lane were chosen as a sample of information to study further. For each position, cells were tracked manually to observe 3 main phenotypes. The first one is timing of death, which was based on tracking the time that the cell wall was rupture. Although cells could have been apoptotic for some time before or for various reasons, this was a common point to identify when a cell was dead. The second phenotype is gain in motility that resulted in the end of tracking, for example the timing when cells moved out of their trenches. The third phenotype tracked was cell division, which was suspected to indicate how happy cells were in the device. Using these "times" of relevant events, we compared the different conditions tested to identify the more favorable ones to have Jurkat cells thriving. The graphics in sections 3.3.1-3.3.3 were then generated with R using these timings.

[1] K. Pardee *et al.*, “Rapid, Low-Cost Detection of Zika Virus Using Programmable Biomolecular Components,” *Cell*, vol. 165, no. 5, pp. 1255–1266, May 2016, doi: 10.1016/j.cell.2016.04.059.

[2] F. Caliendo, M. Dukhinova, and V. Siciliano, “Engineered Cell-Based Therapeutics: Synthetic Biology Meets Immunology,” *Front. Bioeng. Biotechnol.*, vol. 7, p. 43, Mar. 2019, doi: 10.3389/fbioe.2019.00043.

[3] V. Chubukov, A. Mukhopadhyay, C. J. Petzold, J. D. Keasling, and H. G. Martín, “Synthetic and systems biology for microbial production of commodity chemicals,” *Npj Syst. Biol. Appl.*, vol. 2, no. 1, p. 16009, Apr. 2016, doi: 10.1038/npjsba.2016.9.

[4] M. T. Pervez, M. J. U. Hasnain, S. H. Abbas, M. F. Moustafa, N. Aslam, and S. S. M. Shah, “A Comprehensive Review of Performance of Next-Generation Sequencing Platforms,” *BioMed Res. Int.*, vol. 2022, pp. 1–12, Sep. 2022, doi: 10.1155/2022/3457806.

[5] A. Hoose, R. Vellacott, M. Storch, P. S. Freemont, and M. G. Ryadnov, “DNA synthesis technologies to close the gene writing gap,” *Nat. Rev. Chem.*, vol. 7, no. 3, pp. 144–161, Jan. 2023, doi: 10.1038/s41570-022-00456-9.

[6] M. Jinek, K. Chylinski, I. Fonfara, M. Hauer, J. A. Doudna, and E. Charpentier, “A Programmable Dual-RNA–Guided DNA Endonuclease in Adaptive Bacterial Immunity,” *Science*, vol. 337, no. 6096, pp. 816–821, Aug. 2012, doi: 10.1126/science.1225829.

[7] T. S. Gardner, C. R. Cantor, and J. J. Collins, “Construction of a genetic toggle switch in Escherichia coli,” *Nature*, vol. 403, no. 6767, pp. 339–342, Jan. 2000, doi: 10.1038/35002131.

[8] M. B. Elowitz and S. Leibler, “A synthetic oscillatory network of transcriptional regulators,” *Nature*, vol. 403, no. 6767, pp. 335–338, Jan. 2000, doi: 10.1038/35002125.

[9] D. T. Riglar *et al.*, “Bacterial variability in the mammalian gut captured by a single-cell synthetic oscillator,” *Nat. Commun.*, vol. 10, no. 1, p. 4665, Oct. 2019, doi: 10.1038/s41467-019-12638-z.

[10] M. Lawson and J. Elf, “Imaging-based screens of pool-synthesized cell libraries,” *Nat. Methods*, vol. 18, no. 4, pp. 358–365, Apr. 2021, doi: 10.1038/s41592-020-01053-8.

[11] Daniel D Shoemaker, Deval A. Lashkari, Don Morris, Mike Mittmann, and Ronald W. Davis, “Quantitative phenotypic analysis of yeast deletion mutants using a highly parallel molecular bar–coding strategy”.

[12] N. Burns *et al.*, “Large-scale analysis of gene expression, protein localization, and gene dlsrupuon in Saccharomyces cerevisiae”.

[13] B. L. Menasche, L. Crisman, D. R. Gulbranson, E. M. Davis, H. Yu, and J. Shen, “Fluorescence Activated Cell Sorting (FACS) in Genome-Wide Genetic Screening of Membrane Trafficking,” *Curr. Protoc. Cell Biol.*, vol. 82, no. 1, Mar. 2019, doi: 10.1002/cpcb.68.

[14] Y. Khilko, P. D. Weyman, J. I. Glass, M. D. Adams, M. A. McNeil, and P. B. Griffin, “DNA assembly with error correction on a droplet digital microfluidics platform,” *BMC Biotechnol.*, vol. 18, no. 1, p. 37, Dec. 2018, doi: 10.1186/s12896-018-0439-9.

[15] S. C. C. Shih *et al.*, “A Versatile Microfluidic Device for Automating Synthetic Biology,” *ACS Synth. Biol.*, vol. 4, no. 10, pp. 1151–1164, 2015, doi: 10.1021/acssynbio.5b00062.

[16] G. Graham *et al.*, “Genome-scale transcriptional dynamics and environmental biosensing,” *Proc. Natl. Acad. Sci.*, vol. 117, no. 6, pp. 3301–3306, Feb. 2020, doi: 10.1073/pnas.1913003117.

[17] E. Z. Macosko *et al.*, “Highly Parallel Genome-wide Expression Profiling of Individual Cells Using Nanoliter Droplets,” *Cell*, vol. 161, no. 5, pp. 1202–1214, May 2015, doi: 10.1016/j.cell.2015.05.002.

[18] K. Jager and K. Jager, “Prion Propagation and Loss in Single Bacterial Cells Concordia University,” no. January, 2022.

[19] P. Wang *et al.*, “Robust growth of escherichia coli,” *Curr. Biol.*, vol. 20, no. 12, pp. 1099–1103, 2010, doi: 10.1016/j.cub.2010.04.045.

[20] F. Zhang, Y. Sun, and C. Luo, “Microfluidic approaches for synthetic gene circuits’ construction and analysis,” *Quant. Biol.*, vol. 9, no. 1, p. 47, 2021, doi: 10.15302/j-qb-021-0235.

[21] M. J. Lawson, D. Camsund, J. Larsson, Ö. Baltekin, D. Fange, and J. Elf, “*In situ* genotyping of a pooled strain library after characterizing complex phenotypes,” *Mol. Syst. Biol.*, vol. 13, no. 10, p. 947, Oct. 2017, doi: 10.15252/msb.20177951.

[22] S. Luro, L. Potvin-Trottier, B. Okumus, and J. Paulsson, “Isolating live cells after high-throughput, long-term, time-lapse microscopy,” *Nat. Methods*, vol. 17, no. 1, pp. 93–100, 2020, doi: 10.1038/s41592-019-0620-7.

[23] A. Seita, H. Nakaoka, R. Okura, and Y. Wakamoto, “Intrinsic growth heterogeneity of mouse leukemia cells underlies differential susceptibility to a growth-inhibiting anticancer drug,” *PLoS ONE*, vol. 16, no. 2 February, pp. 1–16, 2021, doi: 10.1371/journal.pone.0236534.

[24] S. Pearl Mizrahi, O. Gefen, I. Simon, and N. Q. Balaban, “Persistence to anti-cancer treatments in the stationary to proliferating transition,” *Cell Cycle*, vol. 15, no. 24, pp. 3442–3453, 2016, doi: 10.1080/15384101.2016.1248006.

[25] A. Mocciaro *et al.*, "Light-activated cell identification and sorting (LACIS) for selection of edited clones on a nanofluidic device," *Commun. Biol.*, vol. 1, no. 1, 2018, doi: 10.1038/s42003-018-0034-6.

[26] R. Ramji, V. C. Wong, A. K. Chavali, L. M. Gearhart, and K. Miller-Jensen, "A passive-flow microfluidic device for imaging latent HIV activation dynamics in single T cells," *Integr. Biol. U. K.*, vol. 7, no. 9, pp. 998–1010, 2015, doi: 10.1039/c5ib00094g.

[27] K. Chung, C. A. Rivet, M. L. Kemp, and H. Lu, "Imaging Single-Cell Signaling Dynamics with a Deterministic High-Density Single-Cell Trap Array," *Anal. Chem.*, vol. 83, no. 18, pp. 7044–7052, Sep. 2011, doi: 10.1021/ac2011153.

[28] M. A. Unger, H. P. Chou, T. Thorsen, A. Scherer, and S. R. Quake, "Monolithic microfabricated valves and pumps by multilayer soft lithography," *Science*, vol. 288, no. 5463, pp. 113–116, 2000, doi: 10.1126/science.288.5463.113.

[29] L. Potvin-Trottier, S. Luro, and J. Paulsson, "Microfluidics and single-cell microscopy to study stochastic processes in bacteria," *Curr. Opin. Microbiol.*, vol. 43, pp. 186–192, 2018, doi: 10.1016/j.mib.2017.12.004.

[30] A. Ashkin, "Acceleration and Trapping of Particles by Radiation Pressure," *Phys. Rev. Lett.*, vol. 24, no. 4, pp. 156–159, Jan. 1970, doi: 10.1103/PhysRevLett.24.156.

[31] A. Ashkin, J. M. Dziedzic, and T. Yamane, "Optical trapping and manipulation of single cells using infrared laser beams," *Nature*, vol. 330, no. 6150, pp. 769–771, Dec. 1987, doi: 10.1038/330769a0.

[32] A. del Río Hernández, "The process of photolithography to make a microfluidic device." http://biomechanicalregulation-lab.org/photolithography

[33] M. S. Ferry, I. A. Razinkov, and J. Hasty, *Microfluidics for Synthetic Biology*, vol. 497. Elsevier Inc., 2011. doi: 10.1016/b978-0-12-385075-1.00014-7.

[34] Y.-K. Yang and T.-C. Chang, "Experimental analysis and optimization of a photo resist coating process for photolithography in wafer fabrication," *Microelectron. J.*, vol. 37, no. 8, pp. 746–751, Aug. 2006, doi: 10.1016/j.mejo.2005.10.006.

[35] J. W. Lathrop, "The Diamond Ordnance Fuze Laboratory's Photolithographic Approach to Microcircuits," *IEEE Ann. Hist. Comput.*, vol. 35, no. 1, pp. 48–55, Jan. 2013, doi: 10.1109/MAHC.2011.83.

[36] Tirandazi, Pooyan, "Re: How can I align PDMS to PDMS layers? .," 2018. https://www.researchgate.net/post/How-can-I-align-PDMS-to-PDMS-layers/5b9999dd8b950022ef0e8f8e/citation/download.

[37] Rafael Gómez-Sjöberg, "Pressure Control," *Rafael's Microfluidics*. https://sites.google.com/site/rafaelsmicrofluidicspage/valve-controllers/pressure-control

[38] B. Okumus *et al.*, "Microfluidics-Assisted Cell Screening (MACS): an automated platform for single-cell microscopy of suspension cultures Burak," *Nat Protoc*, vol. 13, no. 1, pp. 147–154, 2018, doi: 10.1038/nprot.2017.127.Microfluidics-Assisted.

[39] W. M. Lee, P. J. Reece, R. F. Marchington, N. K. Metzger, and K. Dholakia, "Construction and calibration of an optical trap on a fluorescence optical microscope," *Nat. Protoc.*, vol. 2, no. 12, pp. 3226–3238, 2007, doi: 10.1038/nprot.2007.446.

[40] A. Blázquez-Castro, "Optical tweezers: Phototoxicity and thermal stress in cells and biomolecules," *Micromachines*, vol. 10, no. 8, pp. 1–42, 2019, doi: 10.3390/mi10080507.

[41] J.-B. Lugagne, H. Lin, and M. J. Dunlop, “DeLTA: Automated cell segmentation, tracking, and lineage reconstruction using deep learning,” *PLOS Comput. Biol.*, vol. 16, no. 4, p. e1007673, April. 2020, doi: 10.1371/journal.pcbi.1007673.

[42] C. C. Sachs *et al.*, “Image-Based Single Cell Profiling: High-Throughput Processing of Mother Machine Experiments,” *PLOS ONE*, vol. 11, no. 9, p. e0163453, Sep. 2016, doi: 10.1371/journal.pone.0163453.

[43] T. M. Norman, N. D. Lord, J. Paulsson, and R. Losick, “Memory and modularity in cell-fate decision making,” *Nature*, vol. 503, no. 7477, pp. 481–486, Nov. 2013, doi: 10.1038/nature12804.

[44] Y. Li *et al.*, “Multigenerational silencing dynamics control cell aging,” *Proc. Natl. Acad. Sci.*, vol. 114, no. 42, pp. 11253–11258, Oct. 2017, doi: 10.1073/pnas.1703379114.

[45] T. Yang, J. Peng, Z. Shu, P. K. Sekar, S. Li, and D. Gao, “Determination of the membrane transport properties of jurkat cells with a microfluidic device,” *Micromachines*, vol. 10, no. 12, pp. 1–13, 2019, doi: 10.3390/mi10120832.

[46] M. Cavrois, C. De Noronha, and W. C. Greene, “A sensitive and specific enzyme-based assay detecting HIV-1 virion fusion in primary T lymphocytes,” *Nat. Biotechnol.*, vol. 20, no. 11, pp. 1151–1154, 2002, doi: 10.1038/nbt745.

[47] D. B. Lyle, T. A. Fuchs, J. P. Casamento, C. C. Davis, and M. L. Swicord, “Intracellular calcium signaling by jurkat T-lymphocytes exposed to a 60 hz magnetic field,” *Bioelectromagnetics*, vol. 18, no. 6, pp. 439–445, 1997, doi: 10.1002/(SICI)1521-186X(1997)18:6<439::AID-BEM6>3.0.CO;2-3.

[48] C.-C. Chen, Y. Zhou, C. A. Morris, J. Hou, and L. A. Baker, “Scanning Ion Conductance Microscopy Measurement of Paracellular Channel Conductance in Tight Junctions,” *Anal. Chem.*, vol. 85, no. 7, pp. 3621–3628, Apr. 2013, doi: 10.1021/ac303441n.

[49] K. Tang, C. G. Boudreau, C. M. Brown, and A. Khadra, “Paxillin phosphorylation at serine 273 and its effects on Rac, Rho and adhesion dynamics,” *PLOS Comput. Biol.*, vol. 14, no. 7, p. e1006303, Jul. 2018, doi: 10.1371/journal.pcbi.1006303.

[50] Z. Keckesova *et al.*, “LACTB is a tumour suppressor that modulates lipid metabolism and cell state,” *Nature*, vol. 543, no. 7647, pp. 681–686, Mar. 2017, doi: 10.1038/nature21408.

[51] J. S. Zigler, J. L. Lepe-Zuniga, B. Vistica, and I. Gery, “Analysis of the cytotoxic effects of light-exposed hepes-containing culture medium,” *In Vitro Cell. Dev. Biol.*, vol. 21, no. 5, pp. 282–287, May 1985, doi: 10.1007/BF02620943.

[52] G. Pawelec, A. Borowitz, P. H. Krammer, and P. Wernet, “Constitutive Interleukin 2 Production by the Jurkat Human Leukemic T Cell Line,” *Eur. J. Immunol.*, vol. 12, no. 5, pp. 387–392, 1982, doi: 10.1002/eji.1830120506.

[53] G. Gilmore, “Re: How can I expand a transduced single jurkat cell ?,” 2021. https://www.researchgate.net/post/How_can_I_expand_a_transduced_single_jurkat_cell/6113a806559f23647e2f5225/citation/download

[54] Rafael Gómez-Sjöberg, “Views of the Full System,” *Rafael’s Microfluidics*. https://sites.google.com/site/rafaelsmicrofluidicspage/automated-cell-culture/pictures